Project title: **Innovative lightweight cold-formed steel-concrete composite floor system**
Acronym: **LWT-FLOOR** Project ID: **UIP-2020-02-2964**
5th LWT-FLOOR Project Workshop, Zagreb, 18th-19th December 2025

# Reliability of composite steel - concrete floor system made of built-up cold-formed steel elements

Andrea Rajić; Ivan Lukačević

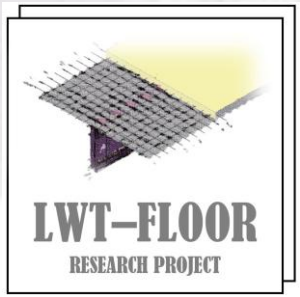



University of Zagreb/Faculty of Civil Engineering
http://www.grad.unizg.hr/lwtfloor

# General

## Introduction

- Motivation
- Objectives and hypothesis
- Research methods

## State of the art

- General
- Shear connection
- Web openings
- Cold-formed steel-concrete composite beams

## Analysis of laboratory research results

- Base material
- Components
- LWT-FLOOR system
- Analysis od laboratory research results of steel and composite beams

## Development and calibration of numerical models

- Material modelling
- Geometric imperfection
- Connection between elements
- Boundary conditions
- Convergence study
- Sensitivity analysis

## Parametric numerical study

- Influence of :
  - steel sheet thickness
  - spot weld density
  - degree of shear connection
  - larger spans
  - different shapes of corrugated web openings

## Analytical proposals

- Overview of analysed analytical methods
- Bending resistance
- Shear resistance
- Restrictions for the calculation

## Probabilistic analysis

- Partial factors based on design values
- Partial factors based on calibration
- Calculation of the partial factor based on design values
- Probabilistic analysis of provided bending resistance models
- Probabilistic parametric sensitivity analyses

## Conclusions

- Scientific contribution of research
- Conclusions of the research
- Recommendations for further research

# Introduction

## Objectives

- to collect and analyse existing reliability verification procedures for composite beams
- to analyse laboratory test results with the identification of failure modes
- to develop and calibrate numerical models based on test results
- to validate deterministically and probabilistically analytical models
- to develop a reliable design procedure for the analysed system

## Hypothesis

**H1:** The application of built-up cold-formed steel beams in a composite structure with reinforced concrete slab can replace hot-rolled steel beams with reduced steel consumption

**H2:** Spot welds and demountable shear connectors will provide a reliable connection between elements of the system.

# Introduction

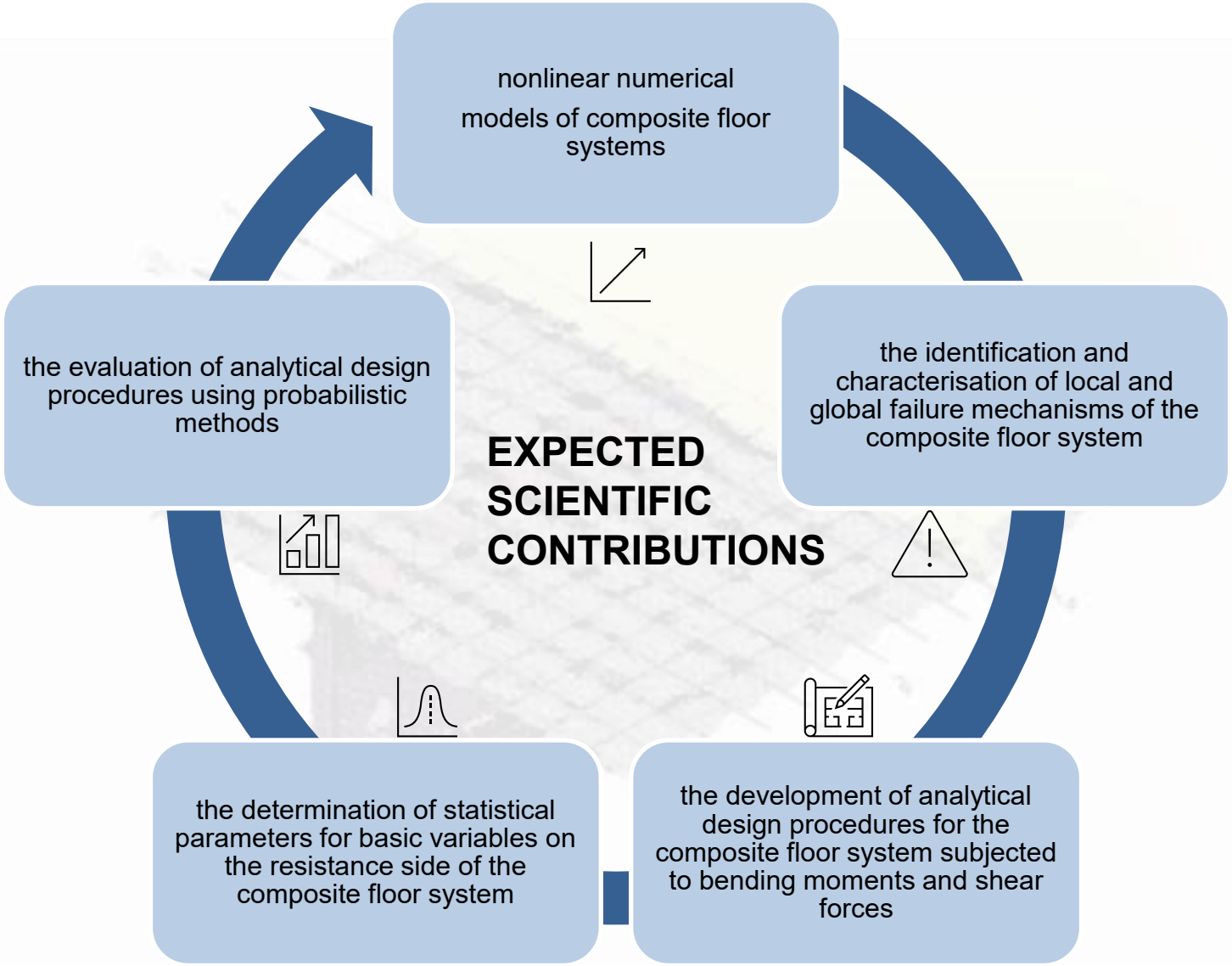

# Introduction

## Research methods

- analytical methods

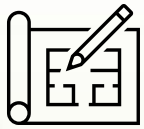

- experimental methods

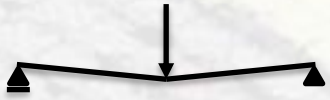

- numerical methods

- probabilistic methods

# State of the art

## Shear connection

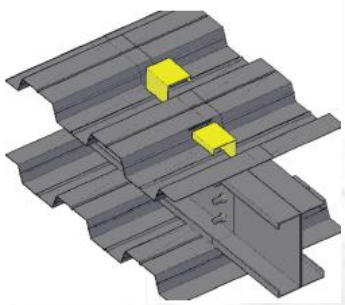

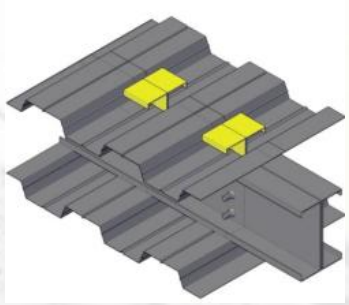

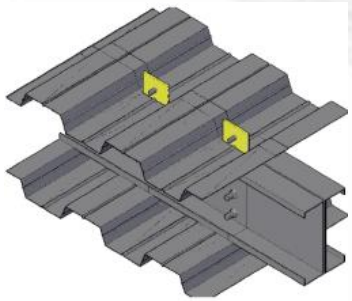

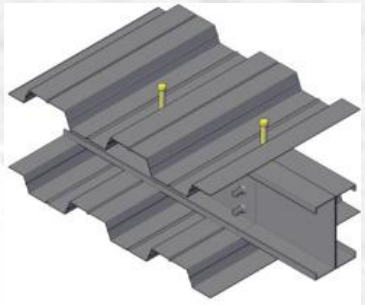

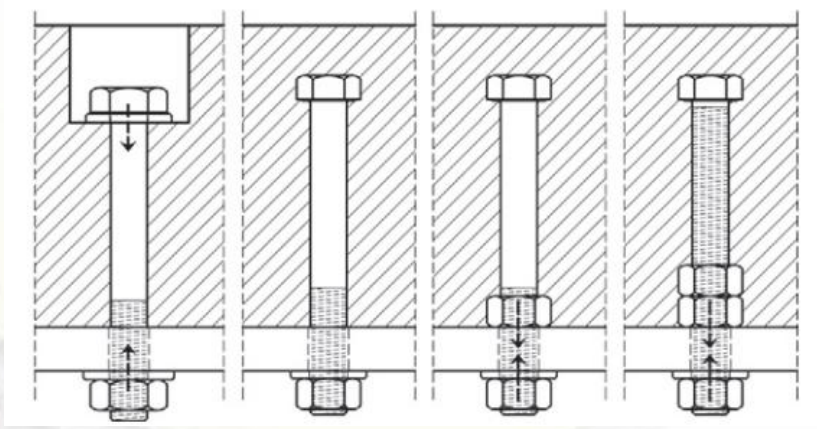

1) Welded shear connectors
   - impossible to dismantle, modify, or recycle the structure's components
   - complicate the reuse, replacement, or repair of parts

2) Demountable shear connectors

# State of the art

## Web openings

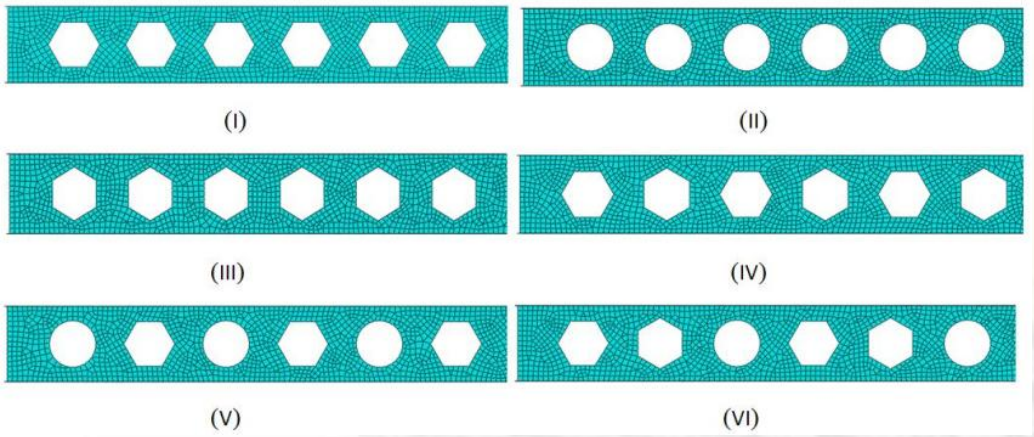



- reduce the cross-sectional area
- affecting bending capacity, shear capacity, and local stability

# State of the art

Advantages of composite steel-concrete systems

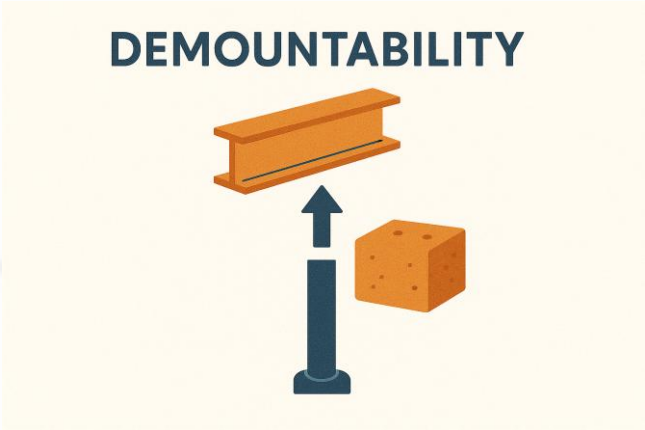


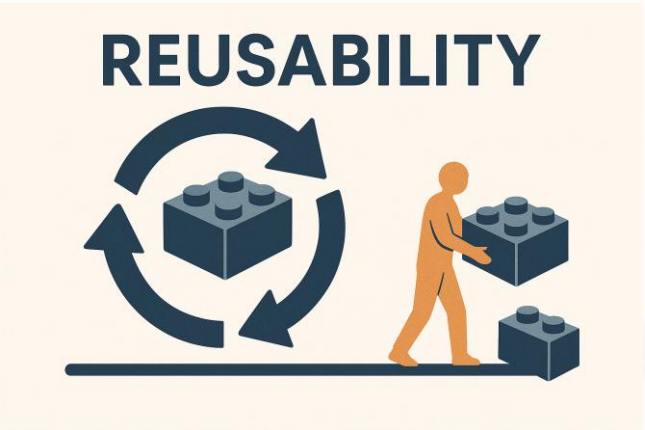


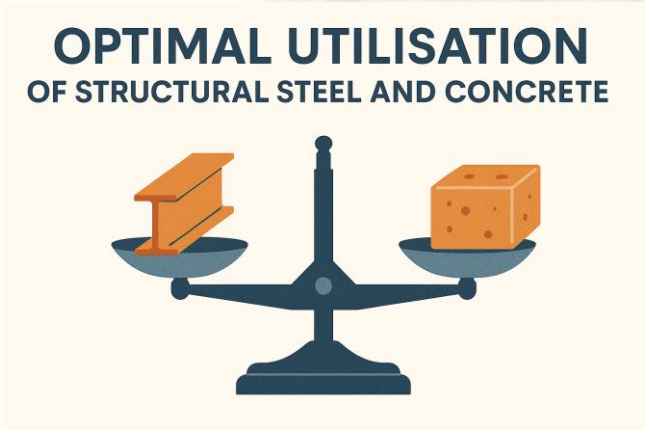


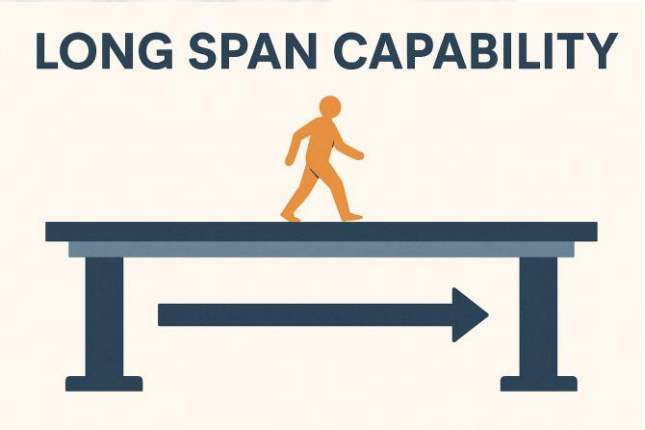

# Analysis of laboratory research results

## BASE MATERIAL

### STEEL SHEETS

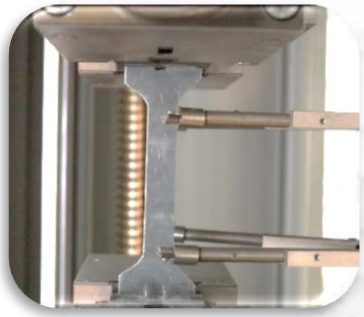

- grade: DX51; S 350 GD
- thickness: 0.8 mm
  - 1.0 mm
  - 1.25 mm
  - 1.5 mm
  - 2.0 mm
  - 2.5 mm
  - 3.0 mm

### BOLTS

- quality: 8.8
- diameter:
  - 12 mm (M12)
  - 16 mm (M16)

### REINFORCEMENT MESH AND BARS

- bars: Ø8 mm
- mesh: Ø10 mm

### CONCRETE CYLINDERS

# Analysis of laboratory research results

## SPOT WELD CHARACTERISTICS

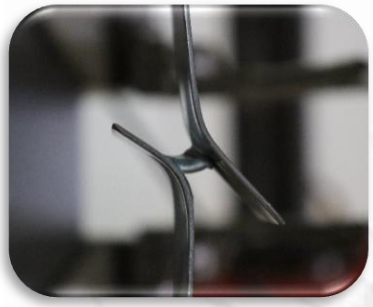

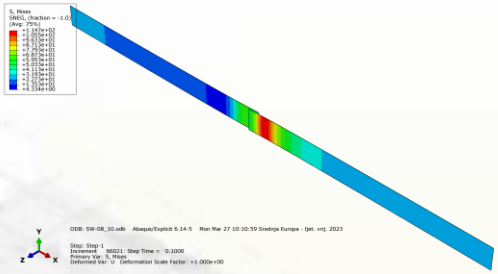

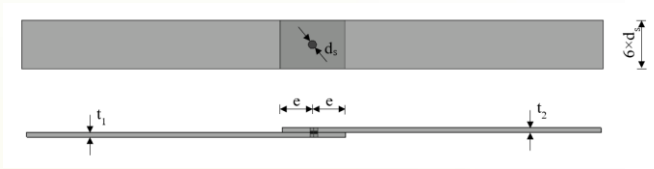


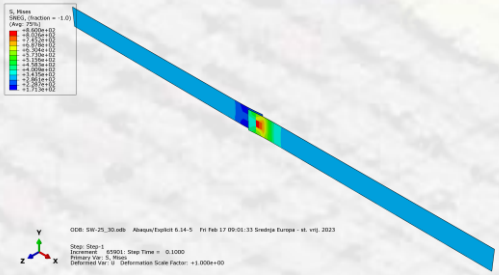

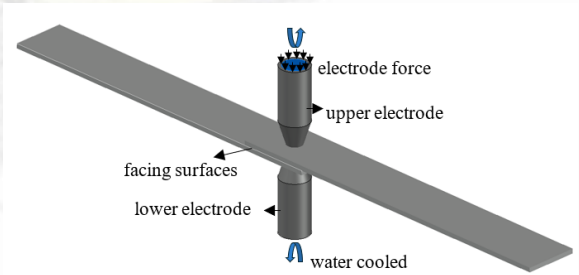


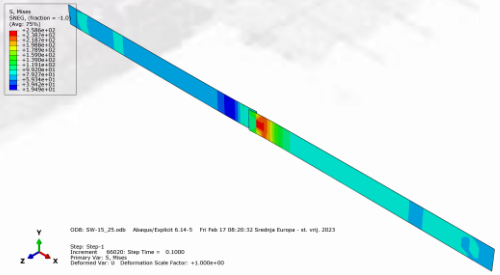

# Analysis of laboratory research results

## LWT-FLOOR SYSTEM

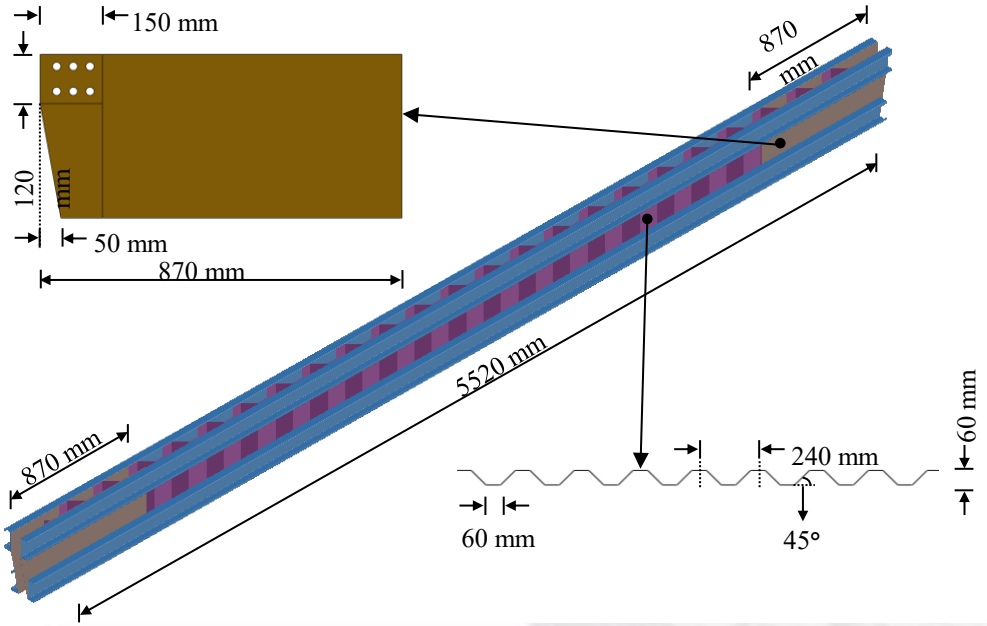


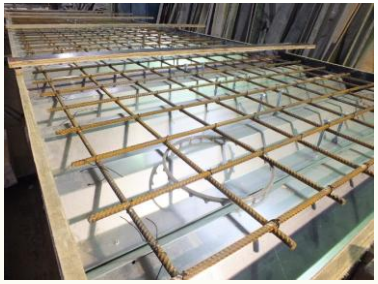

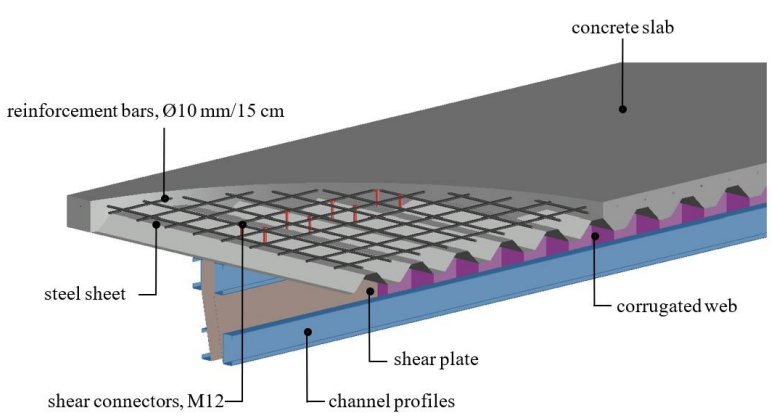


| | Overall height [mm] | Channel thickness [mm] | CW thickness [mm] | SP thickness [mm] |
|---|---|---|---|---|
| B1 | 400 | 2.5 | 1.0 | 1.0 |
| B2 | 500 | 2.0 | 1.0 | 1.0 |
| B3$^{WO}$ | 400 | 3.0 | 1.5 | 1.5 |

# Analysis of laboratory research results

## LWT-FLOOR SYSTEM

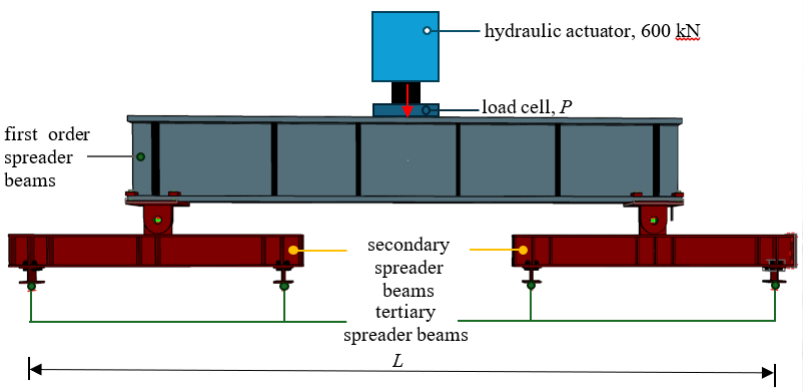


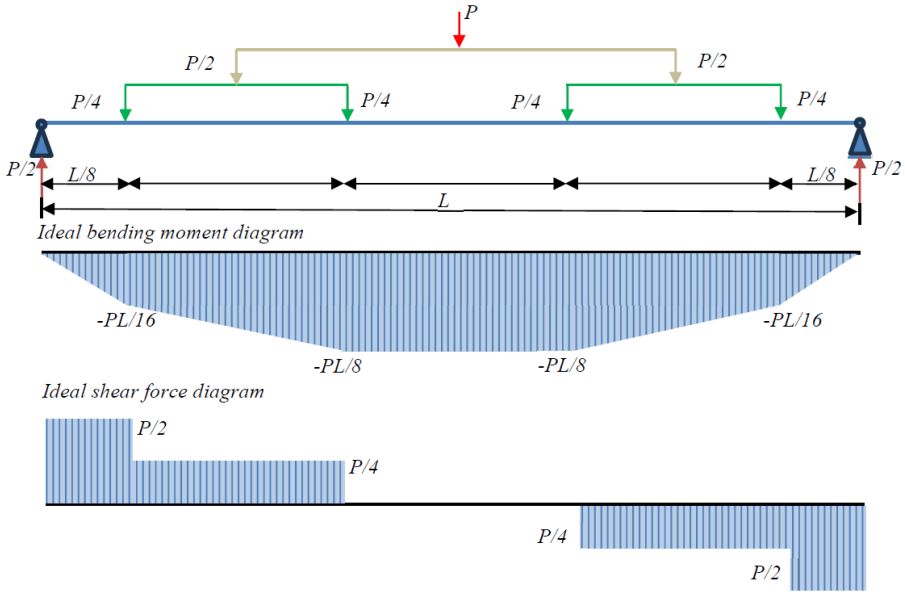


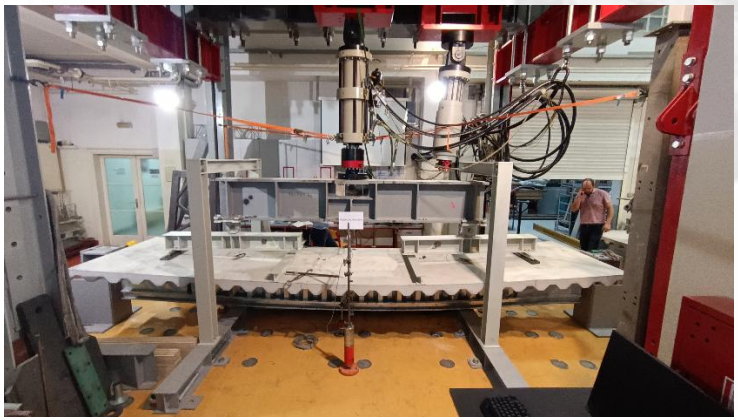

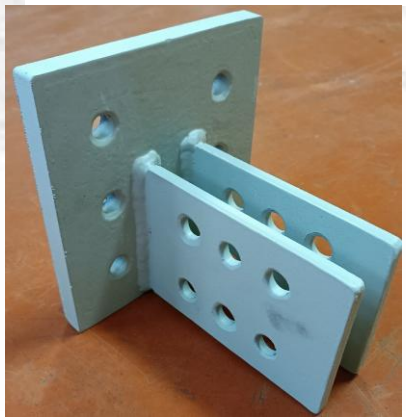

# Analysis of laboratory research results

## LWT-FLOOR SYSTEM

## STEEL BEAM

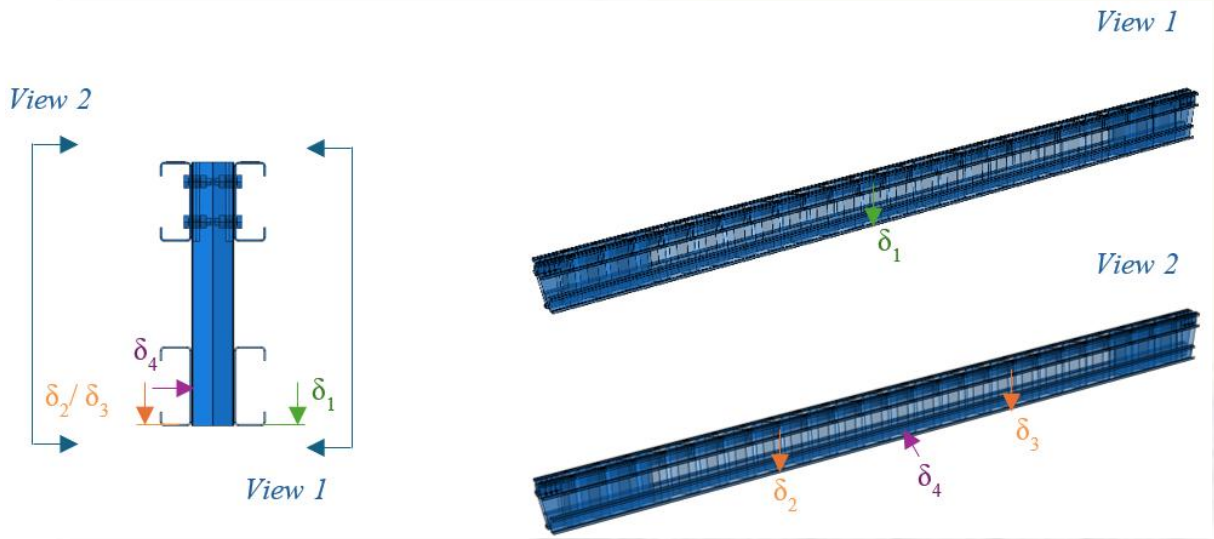


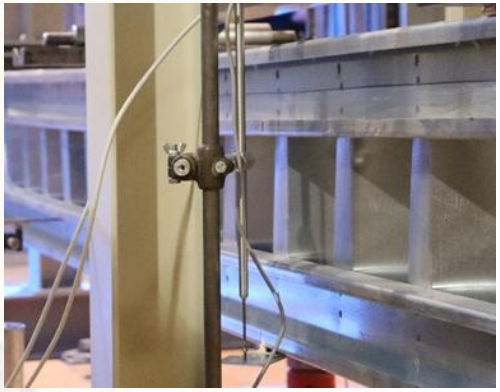

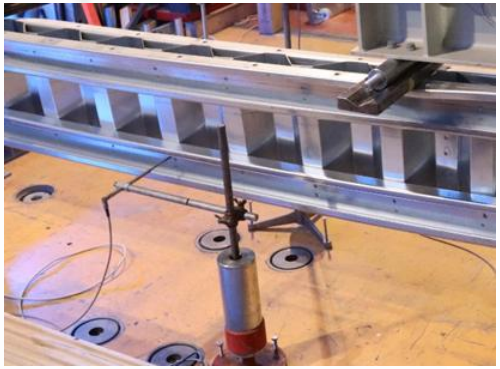

# Analysis of laboratory research results

## LWT-FLOOR SYSTEM

### STEEL BEAM, SB1

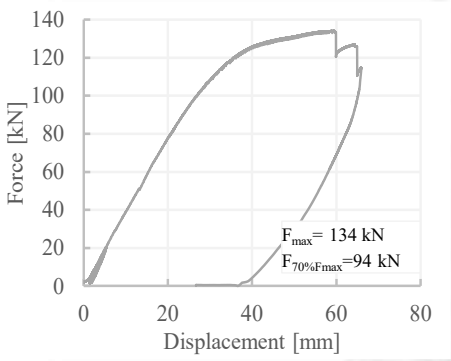


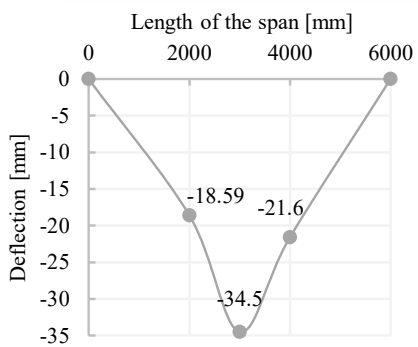


### STEEL BEAM, SB2

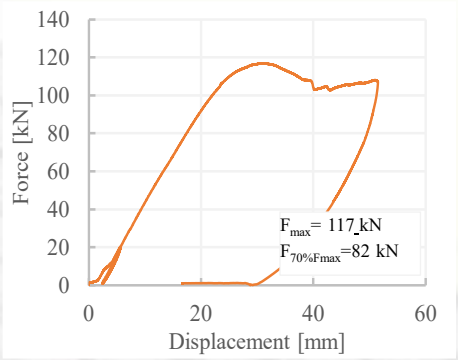


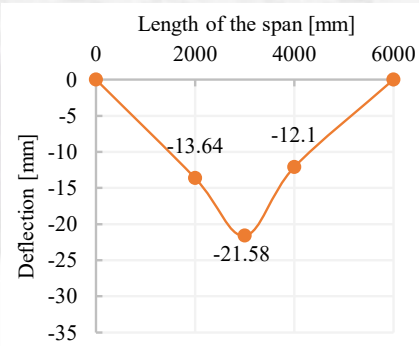


### STEEL BEAM, SB3

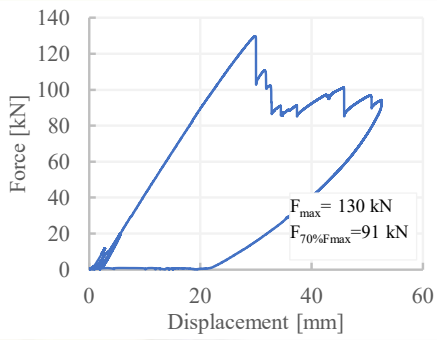


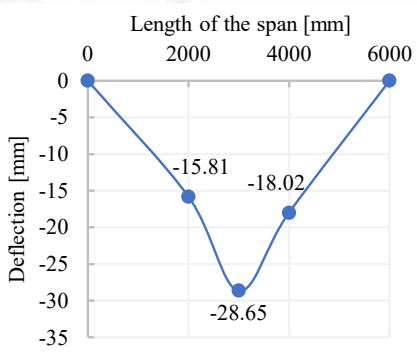

# Analysis of laboratory research results

## LWT-FLOOR SYSTEM

### STEEL BEAM, SB1

- local buckling failure of CS
- lateral deflection - CS buckling
- SP buckling

### STEEL BEAM, SB2

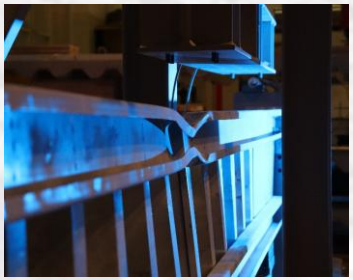

- local buckling of CFS beam under load application points

### STEEL BEAM, SB3

- SW failure

# Analysis of laboratory research results

## LWT-FLOOR SYSTEM

## COMPOSITE BEAM

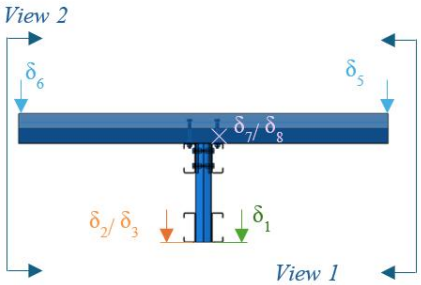


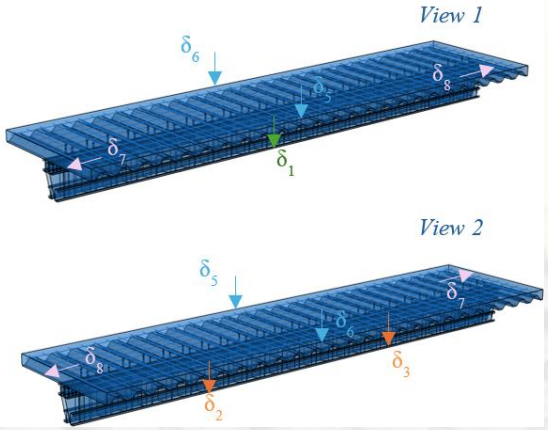


# Analysis of laboratory research results

## LWT-FLOOR SYSTEM

### COMPOSITE BEAM, CB1

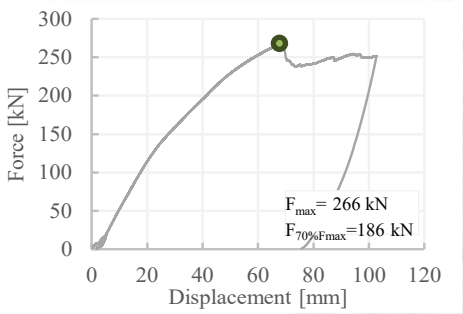


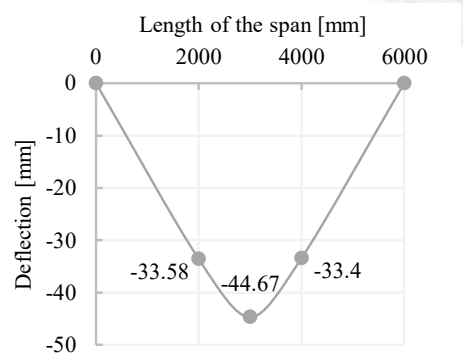


### COMPOSITE BEAM, CB2

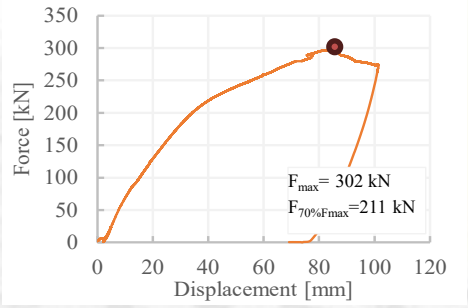


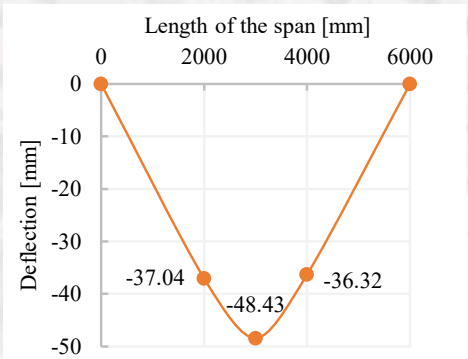


### COMPOSITE BEAM, CB3

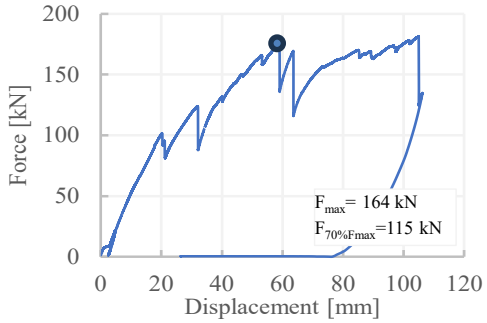


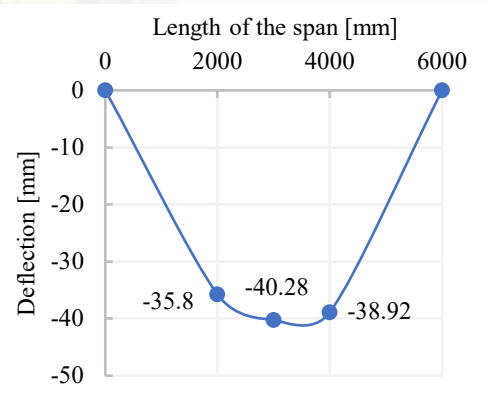

# Analysis of laboratory research results

## LWT-FLOOR SYSTEM

### COMPOSITE BEAM, CB1

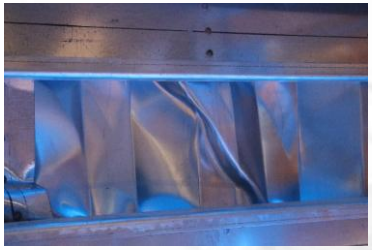

### COMPOSITE BEAM, CB2

### COMPOSITE BEAM, CB3

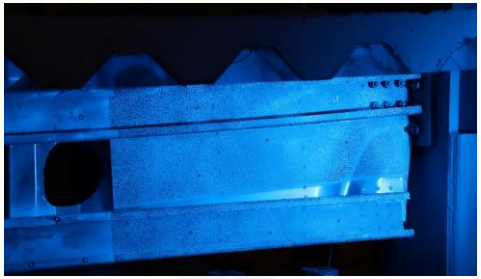

# Development and calibration of numerical models

## STEEL PARTS

### Steel sheets

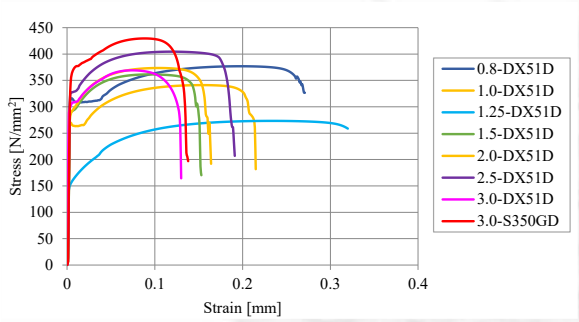


### Bolts

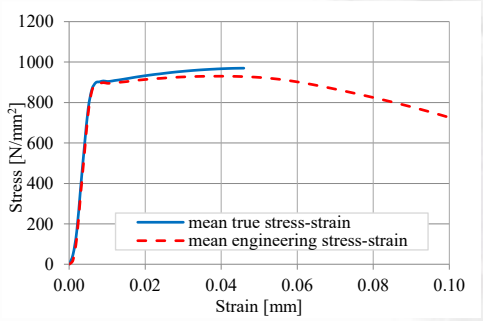


## CONCRETE CYLINDERS

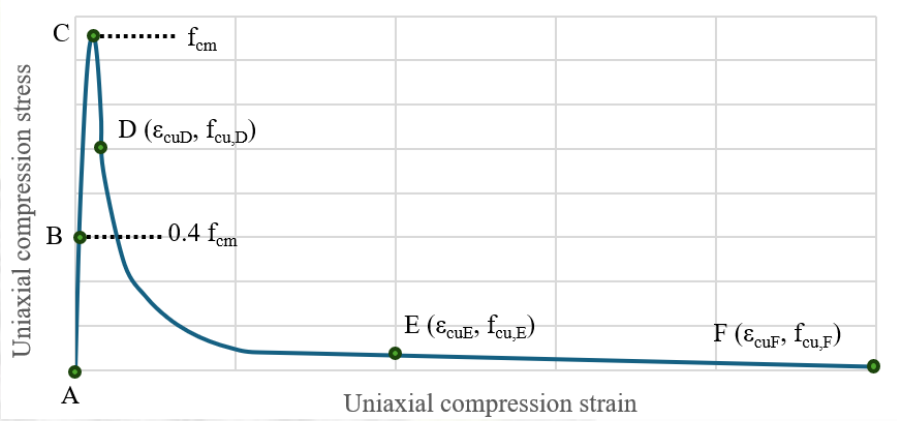


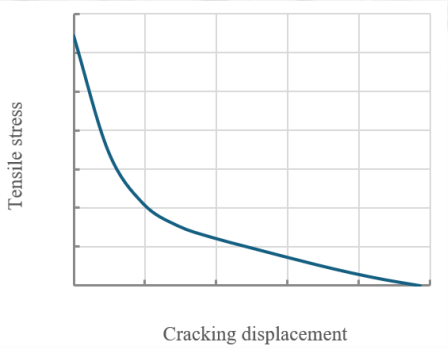


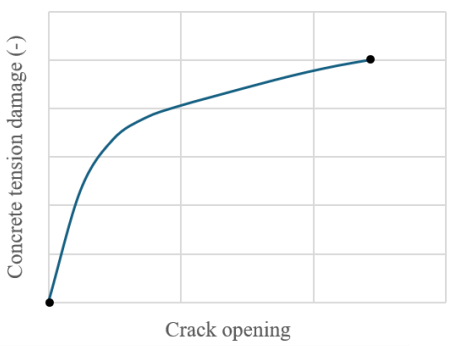

# Development and calibration of numerical models

## GEOMETRIC IMPERFECTIONS



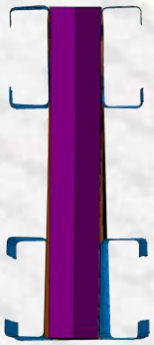

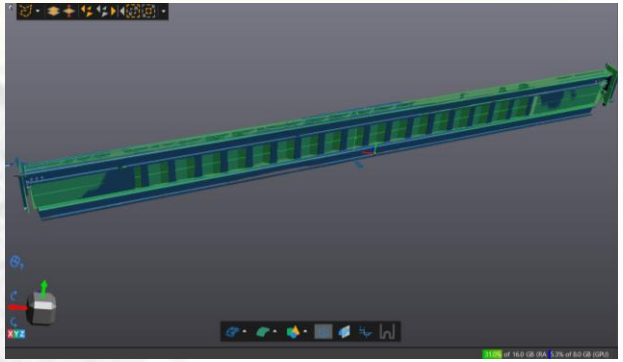

Measured and considered values of deviations

| | Measured deviation [mm] | Considered value in FEM [mm] |
|---|---|---|
| SB1 | 1.905 | 2.0 |
| SB2 | 3.705 | 4.0 |
| SB3 | 3.543 | 4.0 |
| CB1 | 5.728 | 6.0 |
| CB2 | 4.143 | 5.0 |
| CB3 | 5.355 | 6.0 |

# Development and calibration of numerical models

## GEOMETRIC IMPERFECTIONS

## STEEL PARTS

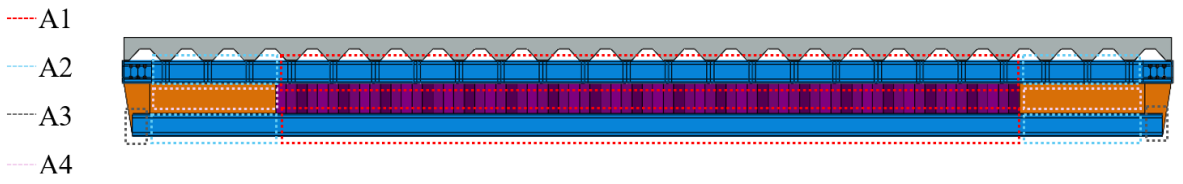


Combinations of spot welds in composite beams

| | CONNECTED ELEMENTS | CB1 | CB2 | CB3 |
|---|---|---|---|---|
| A1 | C-CW | 1.0-2.5 | 1.0-2.0 | 1.5-3.0 |
| A2 | C-CW-SP | 2.5-1.0-1.0 | 2.0-1.0-1.0 | 3.0-1.5-1.5 |
| A3 | C-SP | 1.0-2.5 | 1.0-2.0 | 1.5-3.0 |
| A4 | SP-CW | 1.0-1.0 | 1.0-1.0 | 1.5-1.5 |

## SHEAR CONNECTION

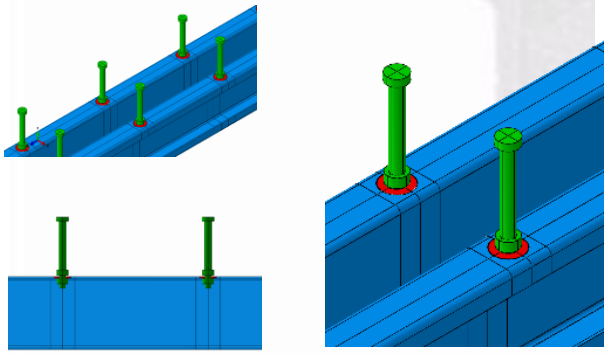

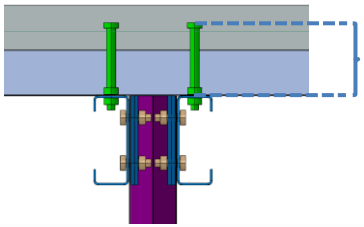

embedded part of shear connectors

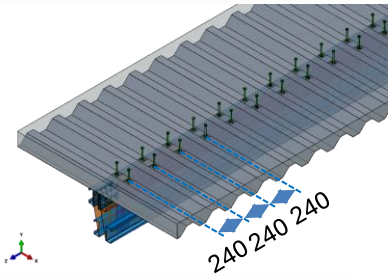

# Development and calibration of numerical models

## CONVERGENCE STUDY

## MESH SIZE

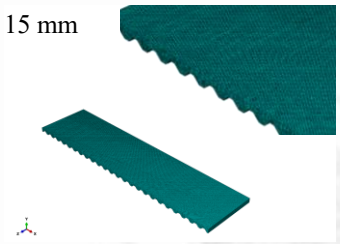


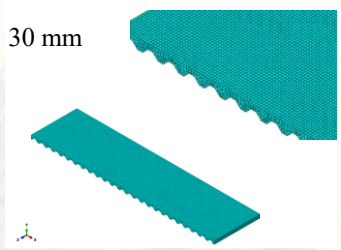


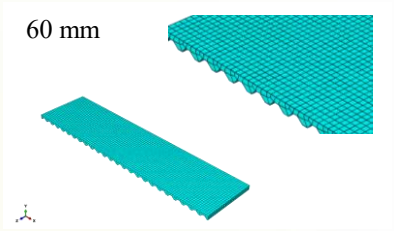


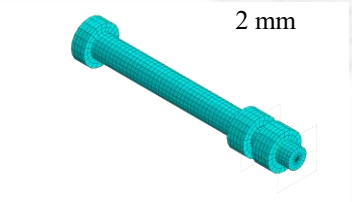


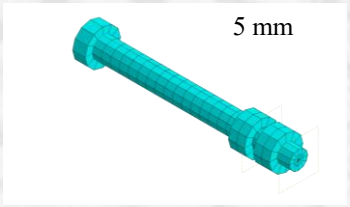


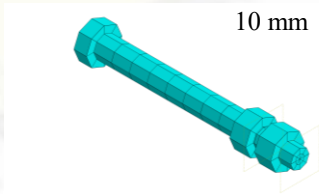


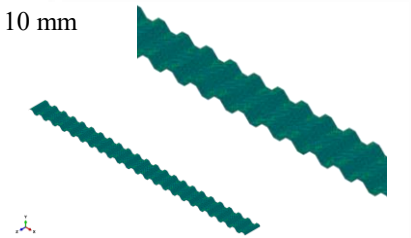


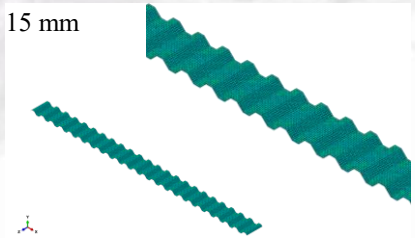


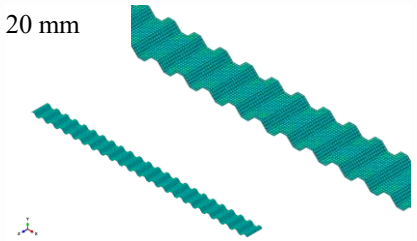

# Development and calibration of numerical models

## CONVERGENCE STUDY

### MASS SCALING FACTOR – ENERGY CHECK

ratio between kinetic energy and internal energy should be in the range of 5% - 10%

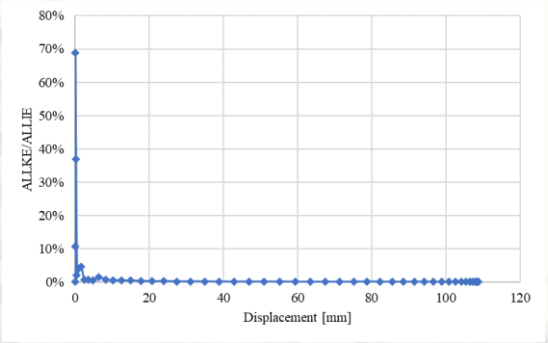


a) model with applied self-weight

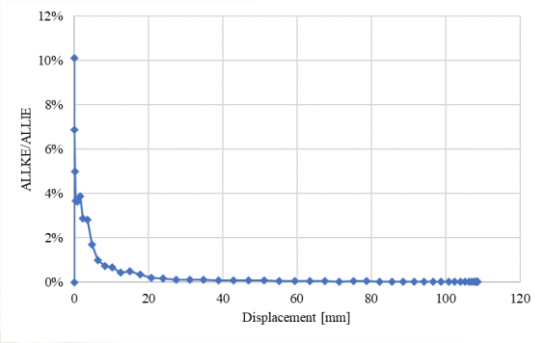


b) model without applied self-weight

The purpose - defining the self-weight can cause energy disorder at the start of the analysis, but it doesn't lead to dynamic effects, as evidenced by the similar shape of the curve for both models

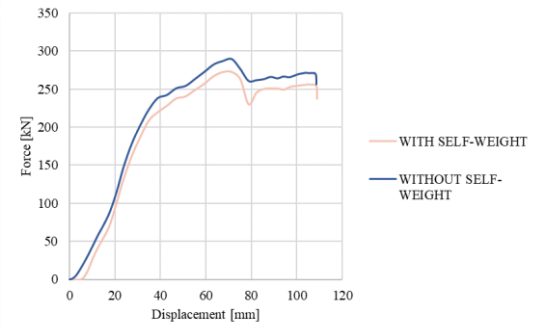

# Development and calibration of numerical models

## CONVERGENCE STUDY

## COMPOSITE BEAM– CB1


| NAME | Ultimate load [kN] EXP | FEM | Ratio EXP/FEM |
|---|---|---|---|
| CB1 | 266 | 272 | 0.98 |

Comparison of the concrete slab slip

| | $\delta_6$ [mm] EXP | FEM | Ratio EXP/FEM | $\delta_7$ [mm] EXP | FEM | Ratio EXP/FEM |
|---|---|---|---|---|---|---|
| CB1 | 3.95 | 3.51 | 1.13 | 4.47 | 5.68 | 0.79 |

in the process of publication

# Development and calibration of numerical models

## CONVERGENCE STUDY

## COMPOSITE BEAM– CB2

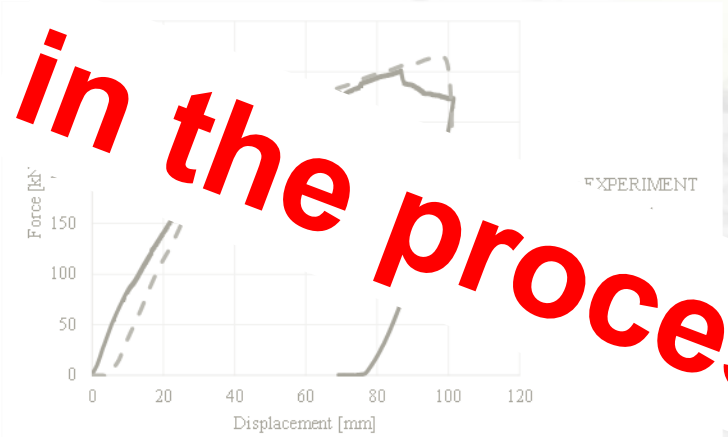


| NAME | Ultimate load [kN] | | Ratio |
|---|---|---|---|
| | EXP | FEM | EXP/FEM |
| CB2 | 302 | 315 | 0.96 |

Comparison of the concrete slab slip

| | $\delta_6$ [mm] | | Ratio | $\delta_7$ [mm] | | Ratio |
|---|---|---|---|---|---|---|
| | EXP | FEM | EXP/FEM | EXP | FEM | EXP/FEM |
| CB2 | 1.45 | 1.50 | 0.97 | 1.25 | 1.85 | 0.68 |

in the process of publication

# Development and calibration of numerical models

## CONVERGENCE STUDY

## COMPOSITE BEAM– CB3

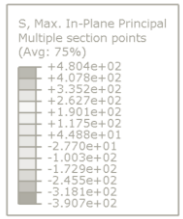


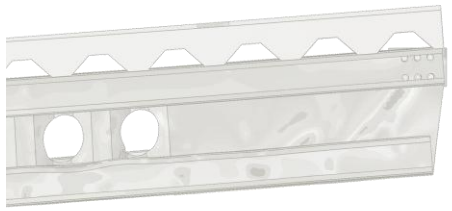

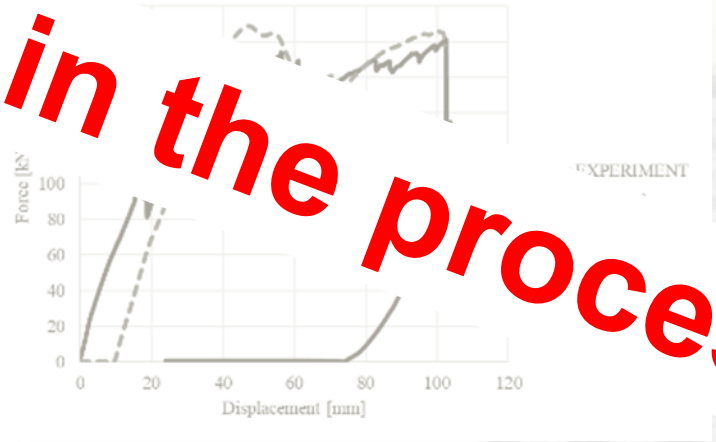


in the process of publication

| NAME | Ultimate load [kN] EXP | FEM | Ratio EXP/FEM |
|---|---|---|---|
| CB3 | 164 | 189 | 0.87 |

Comparison of the concrete slab slip

| | $\delta_6$ [mm] EXP | FEM | Ratio EXP/FEM | $\delta_7$ [mm] EXP | FEM | Ratio EXP/FEM |
|---|---|---|---|---|---|---|
| CB3 | 4.87 | 4.99 | 0.98 | 2.91 | 4.51 | 0.65 |

# Development and calibration of numerical models

## SENSITIVITY ANALYSIS

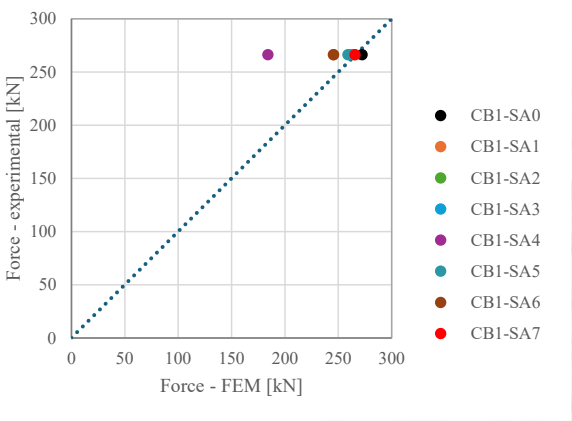


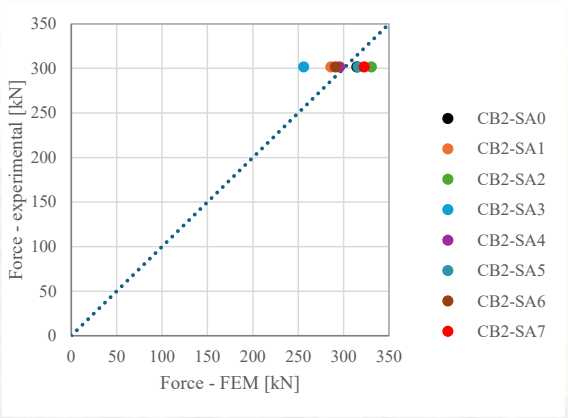


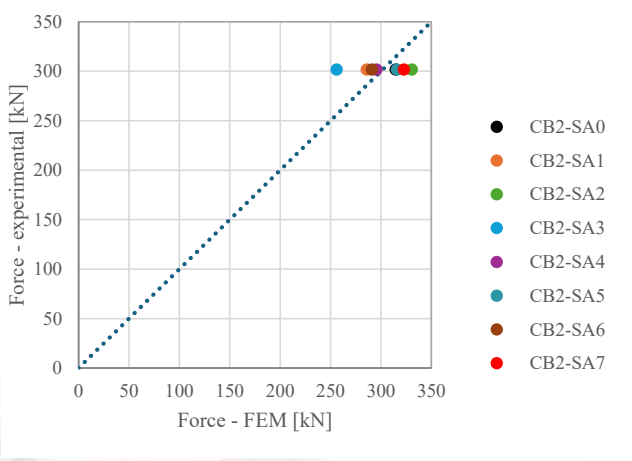


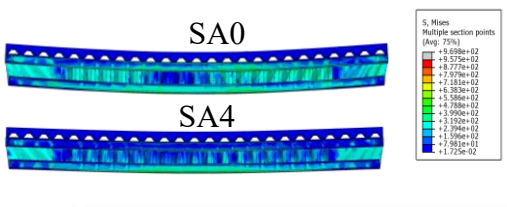


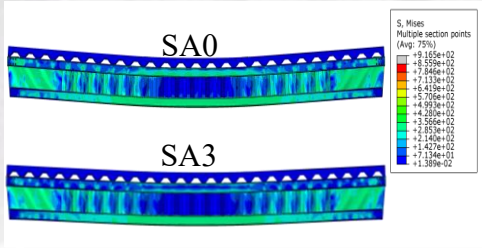


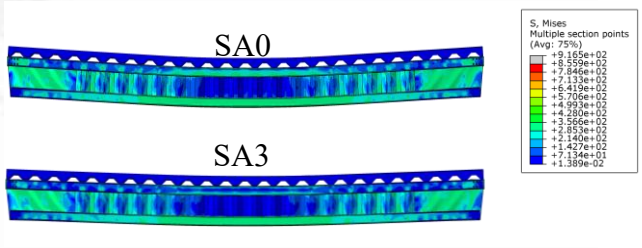

# Parametric numerical study

PARAMETRIC NUMERICAL STUDY

Group 1: Influence of Steel Sheet thickness

Influence of different channel thickness

Influence of different corrugated web thickness

Influence of different shear plate thickness

Group 2: Influence of spot weld density

Group 3: Influence of degree of shear connection

Group 4: Influence of Larger Spans

Group 5: Influence of Different Shapes of Corrugated Web Openings

## PARAMETRIC NUMERICAL STUDY

### Nomenclature

- beam length = 6 m
- steel beam height = 400 mm
- channel profile height of 120 mm and thickness of 3.0 mm
- corrugated web thickness=1.0 mm
- shear plate thickness=1.0 mm

6m_400_C120/3.0_CW1.0_SP1.0_M12_PAIRS_WOC_5SW

additional information about model:

- shear connection achieved by bolts M12 positioned in pairs
- circular shape of web openings
- channel profiles connected to other steel elements by five spot welds in the cross-section

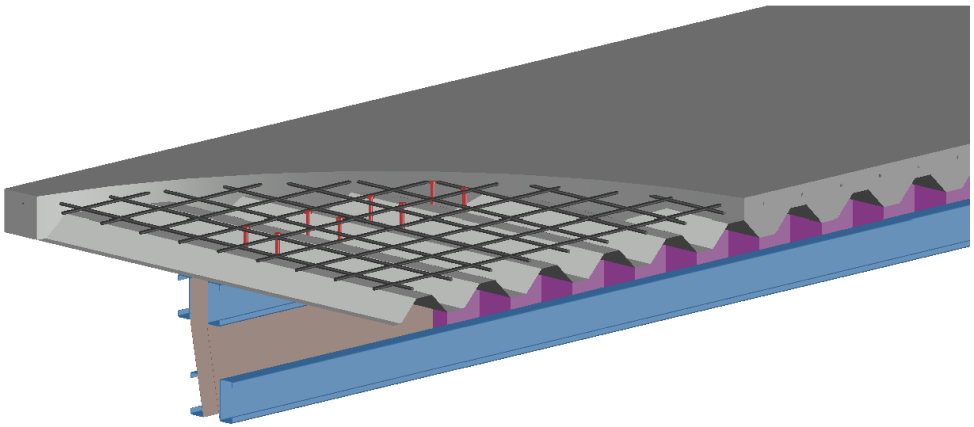

# Parametric numerical study

## Group 1: Influence of Steel Sheet thickness

### Influence of different channel thickness

Influence of steel sheet thickness – steel beam height 400 mm, span 6 m

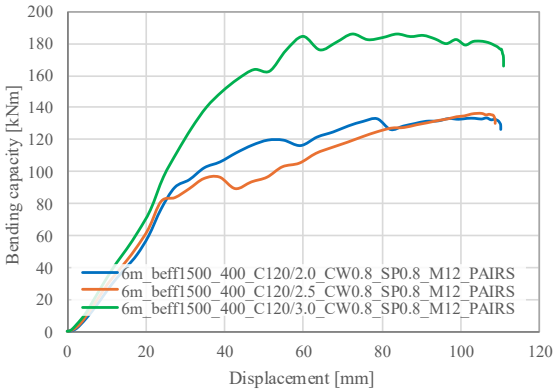


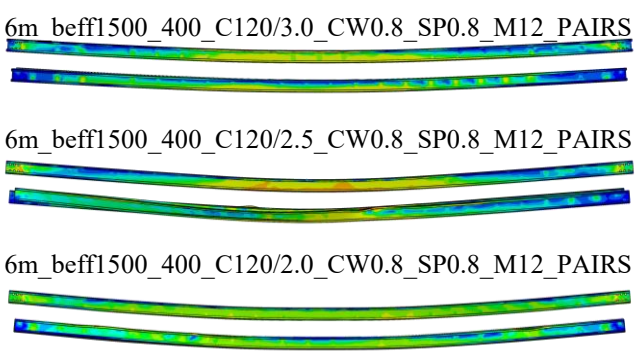


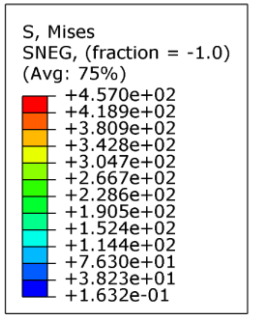


Influence of steel sheet thickness – steel beam height 500 mm, span 6 m

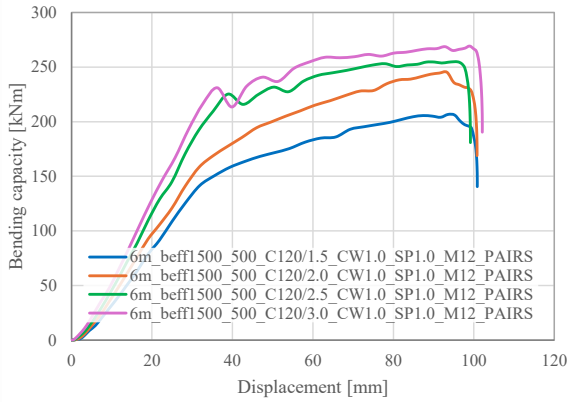


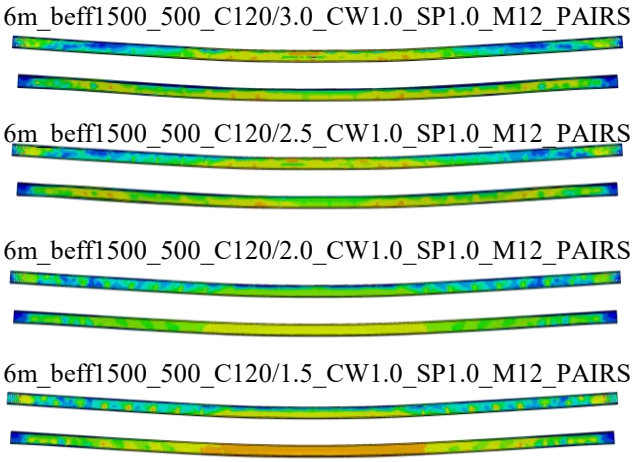


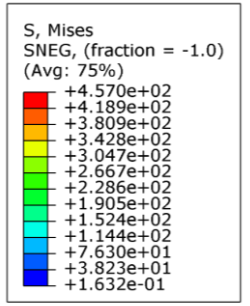

# Parametric numerical study

## Group 1: Influence of Steel Sheet thickness

### Influence of different channel thickness

Influence of corrugated web thickness – steel beam height 400 mm, span 6 m - channel profiles of 2.0 mm

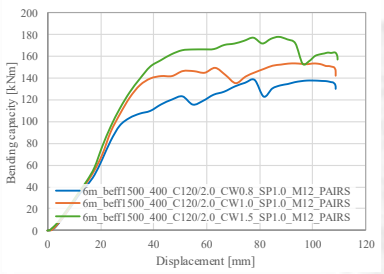


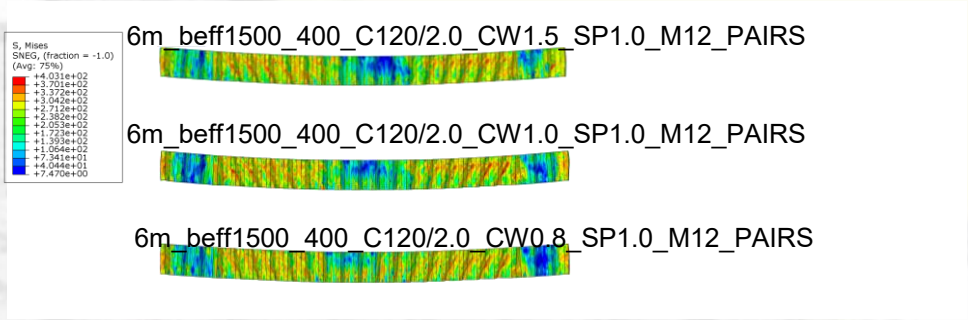


Influence of corrugated web thickness – steel beam height 400 mm, span 6 m - channel profiles of 3.0 mm

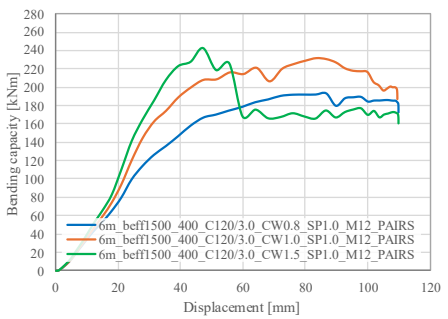


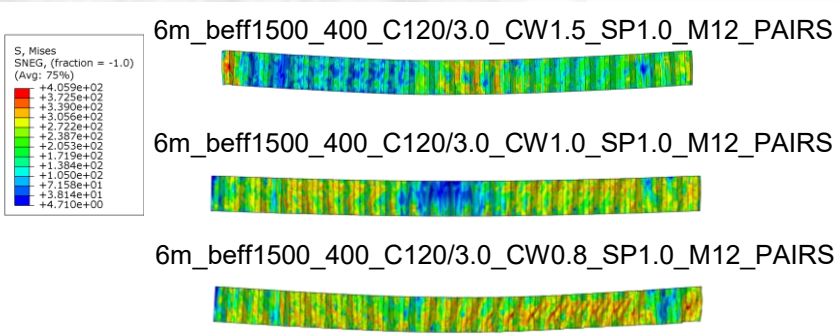

# Parametric numerical study

## Group 1: Influence of Steel Sheet thickness

### Influence of different channel thickness

Influence of corrugated web thickness – steel beam height 500 mm, span 6 m - channel profiles of 1.5 mm

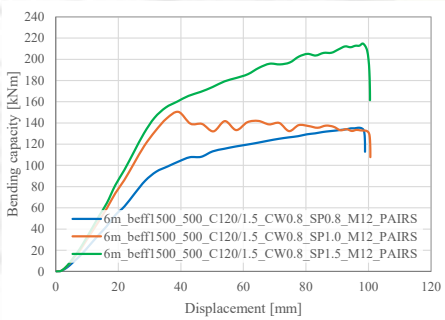


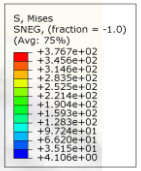


6m_beff1500_500_C120/1.5_CW0.8_SP1.5_M12_PAIRS

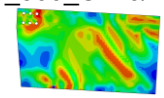

6m_beff1500_500_C120/1.5_CW0.8_SP1.0_M12_PAIRS

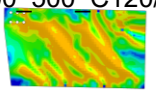

6m_beff1500_500_C120/1.5_CW0.8_SP0.8_M12_PAIRS

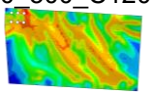

Influence of corrugated web thickness – steel beam height 500 mm, span 6 m - channel profiles of 3.0 mm

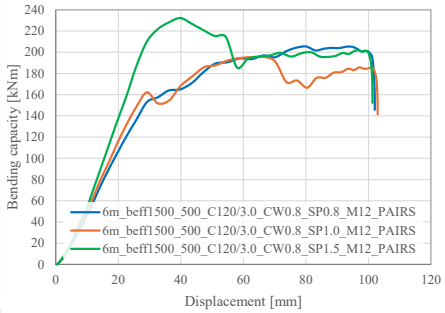


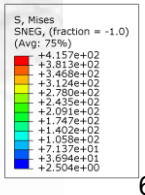


6m_beff1500_500_C120/3.0_CW0.8_SP1.5_M12_PAIRS

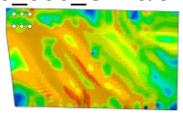

6m_beff1500_500_C120/3.0_CW0.8_SP1.0_M12_PAIRS

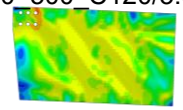

6m_beff1500_500_C120/3.0_CW0.8_SP0.8_M12_PAIRS

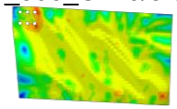

# Parametric numerical study

## PARAMETRIC NUMERICAL STUDY

### Group 2: Influence of spot weld density

span 9 m, concrete slab
effective width 2250 mm

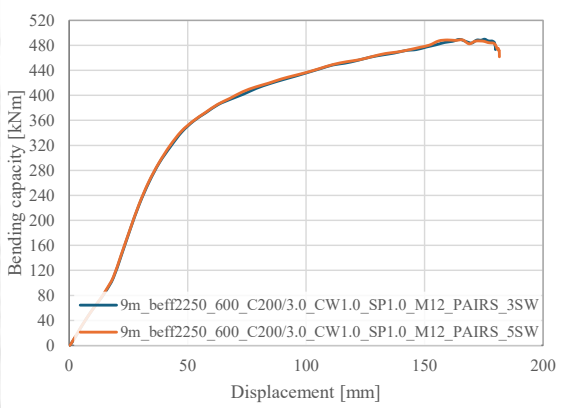


no difference in bending capacity for different numbers of spot welds (3 or 5)

span 12 m, concrete slab
effective width 1500 mm

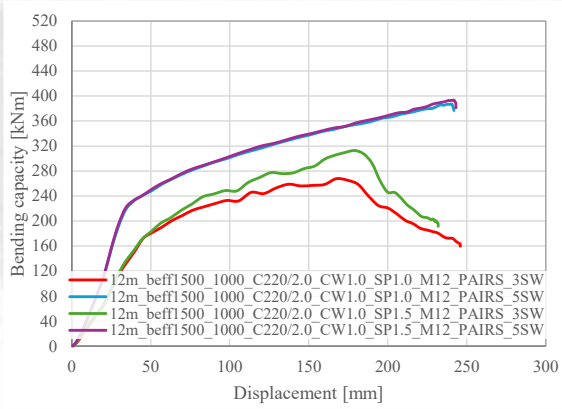


the smaller difference occurs in models with greater shear plate thickness due to the increased resistance of spot welds

# Parametric numerical study

## PARAMETRIC NUMERICAL STUDY

### Group 3: Influence of degree of shear connection

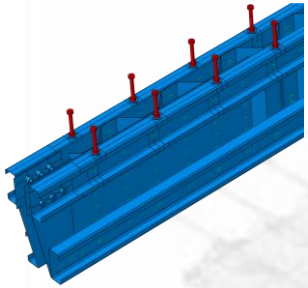

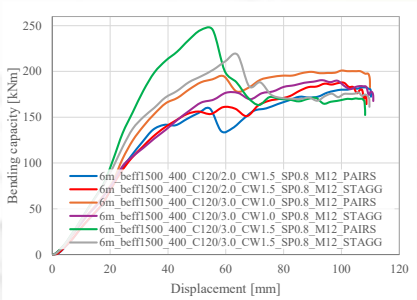


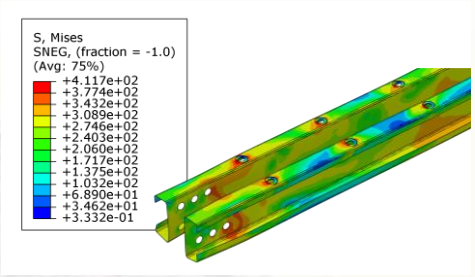


PAIRS

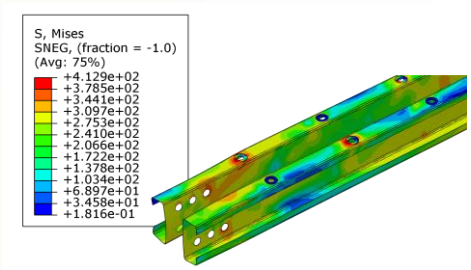


STAGGERED

steel beam height = 400 mm

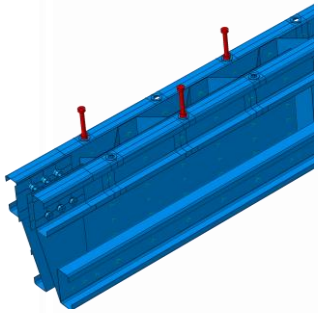

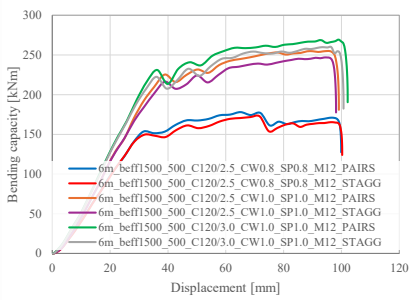


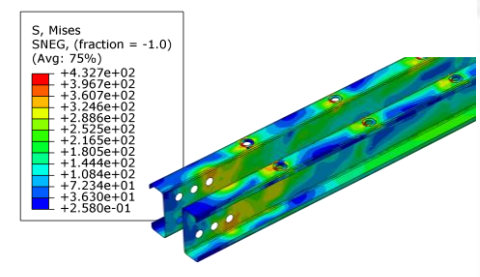


PAIRS

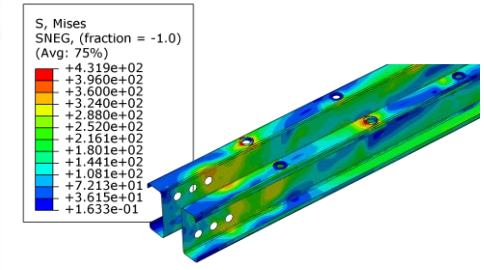


STAGGERED

steel beam height = 500 mm

# Parametric numerical study

## PARAMETRIC NUMERICAL STUDY

### Group 4: Influence of Larger Spans

models with corrugated web thickness and shear plate thickness of 1.0 mm

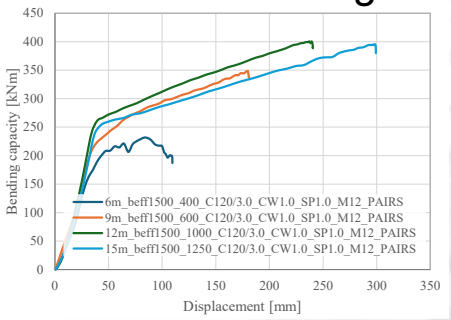


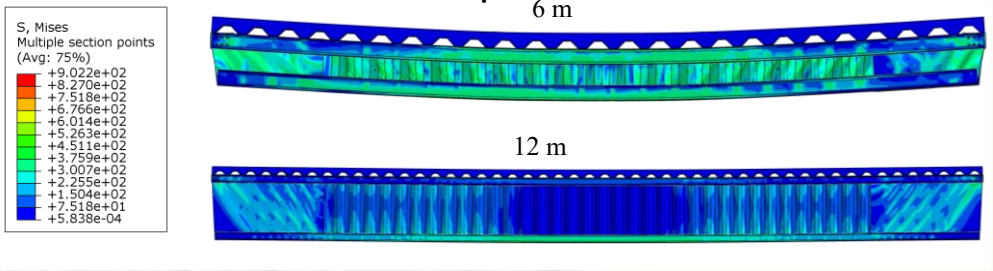


models with corrugated web thickness of 1.5 mm and shear plate thickness of 0.8 mm

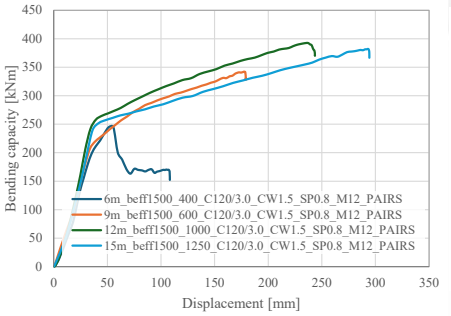


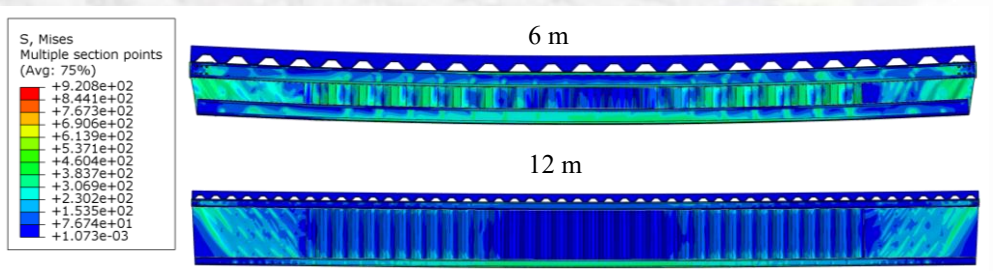

# Parametric numerical study

## Group 4: Influence of Larger Spans

### Influence of different shear plate thickness on 12 m long span

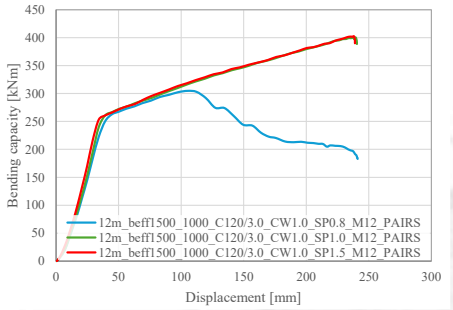


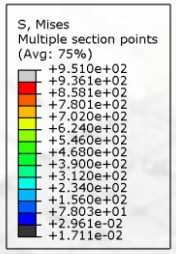


12m_beff1500_1000_C120/3.0_CW1.0_SP0.8_M12_PAIRS

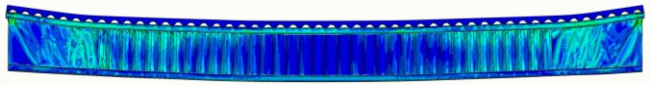

12m_beff1500_1000_C120/3.0_CW1.0_SP1.0_M12_PAIRS

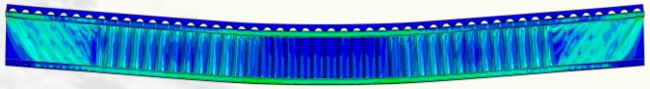

12m_beff1500_1000_C120/3.0_CW1.0_SP1.5_M12_PAIRS

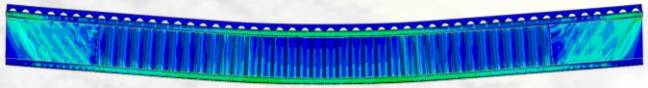

### Influence of different corrugated web thickness on 9 m long span

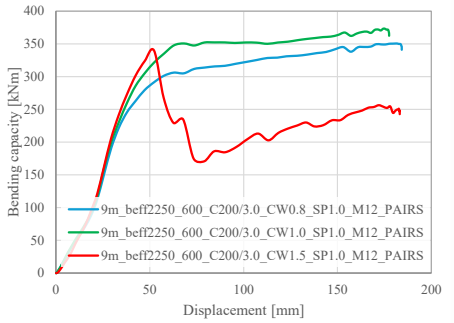


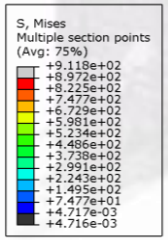


9m_beff2250_600_C200/3.0_CW0.8_SP1.0_M12_PAIRS

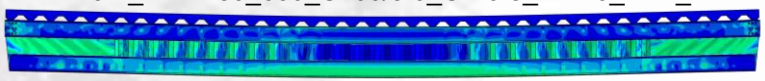

9m_beff2250_600_C200/3.0_CW1.0_SP1.0_M12_PAIRS

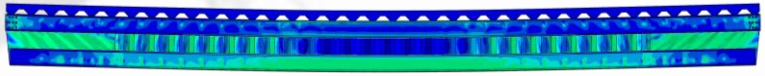

9m_beff2250_600_C200/3.0_CW1.5_SP1.0_M12_PAIRS

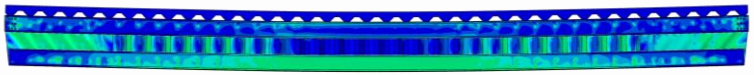

# Parametric numerical study

## Group 5: Influence of Different Shapes of Corrugated Web Openings

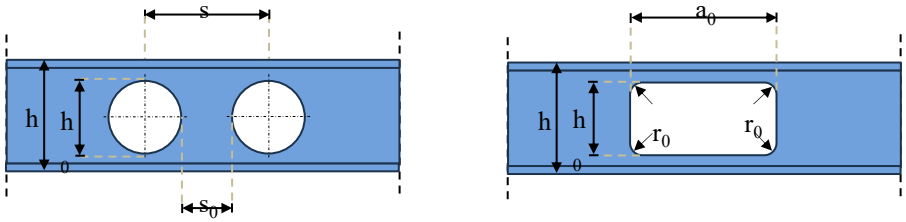


$$\max\ h_0 = 0.8 \cdot h$$

$$\min\ s_0 = 0.1 \cdot h_0$$

$$\max\ h_0 = 0.75 \cdot h$$

$$\max\ a_0 = 2.5 \cdot h_0$$

$$\min\ s_0 = \max(0.5 \cdot a_0;\ h_0)$$

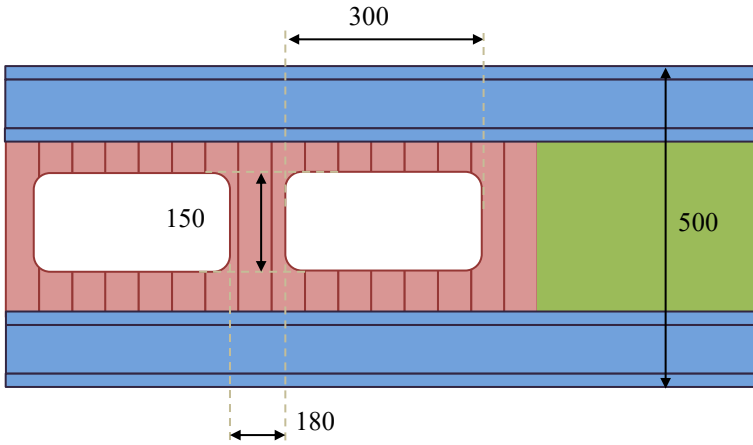


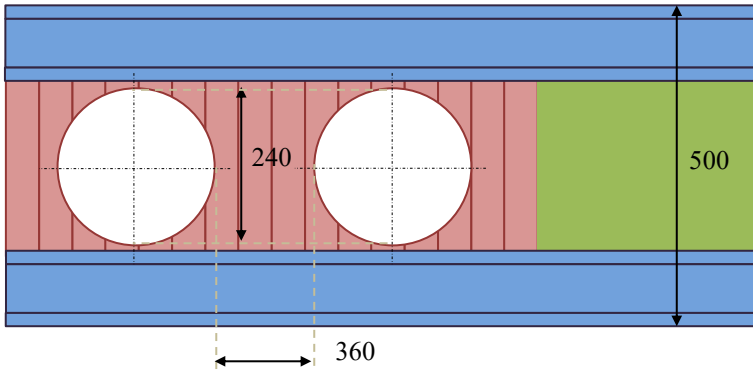

# Parametric numerical study

## Group 5: Influence of Different Shapes of Corrugated Web Openings

### Influence of different shapes of corrugated web openings – channel profile thickness 2.0 mm

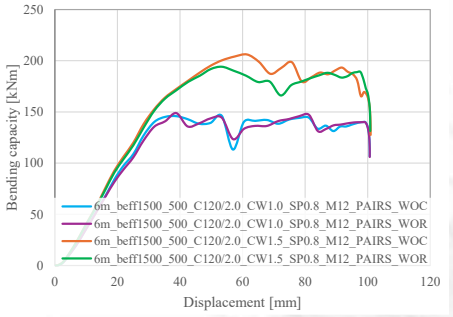


6m_beff1500_500_C120/2.0_CW1.0_SP0.8_M12_PAIRS_WOC

6m_beff1500_500_C120/2.0_CW1.0_SP0.8_M12_PAIRS_WOR

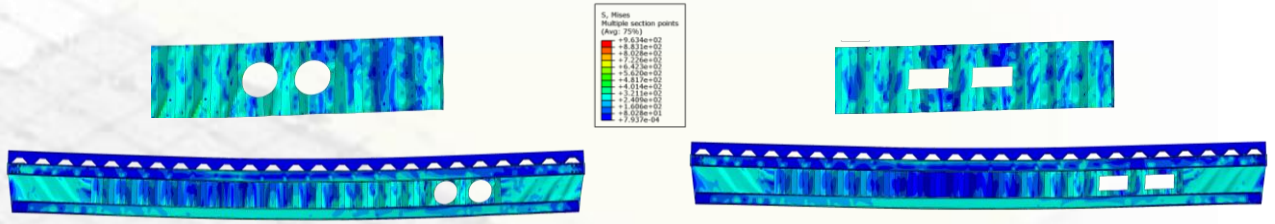

### Influence of different shapes of corrugated web openings – channel profile thickness 3.0 mm

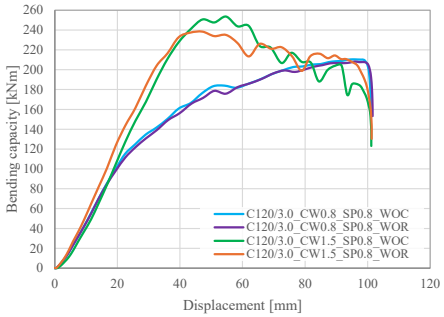


6m_beff1500_500_C120/2.0_CW1.5_SP0.8_M12_PAIRS_WOC

6m_beff1500_500_C120/2.0_CW1.5_SP0.8_M12_PAIRS_WOR

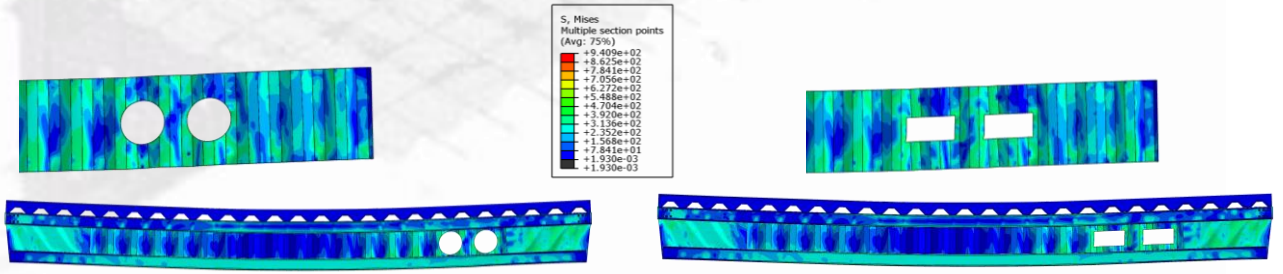

# Analytical proposals

## Overview of analysed analytical methods

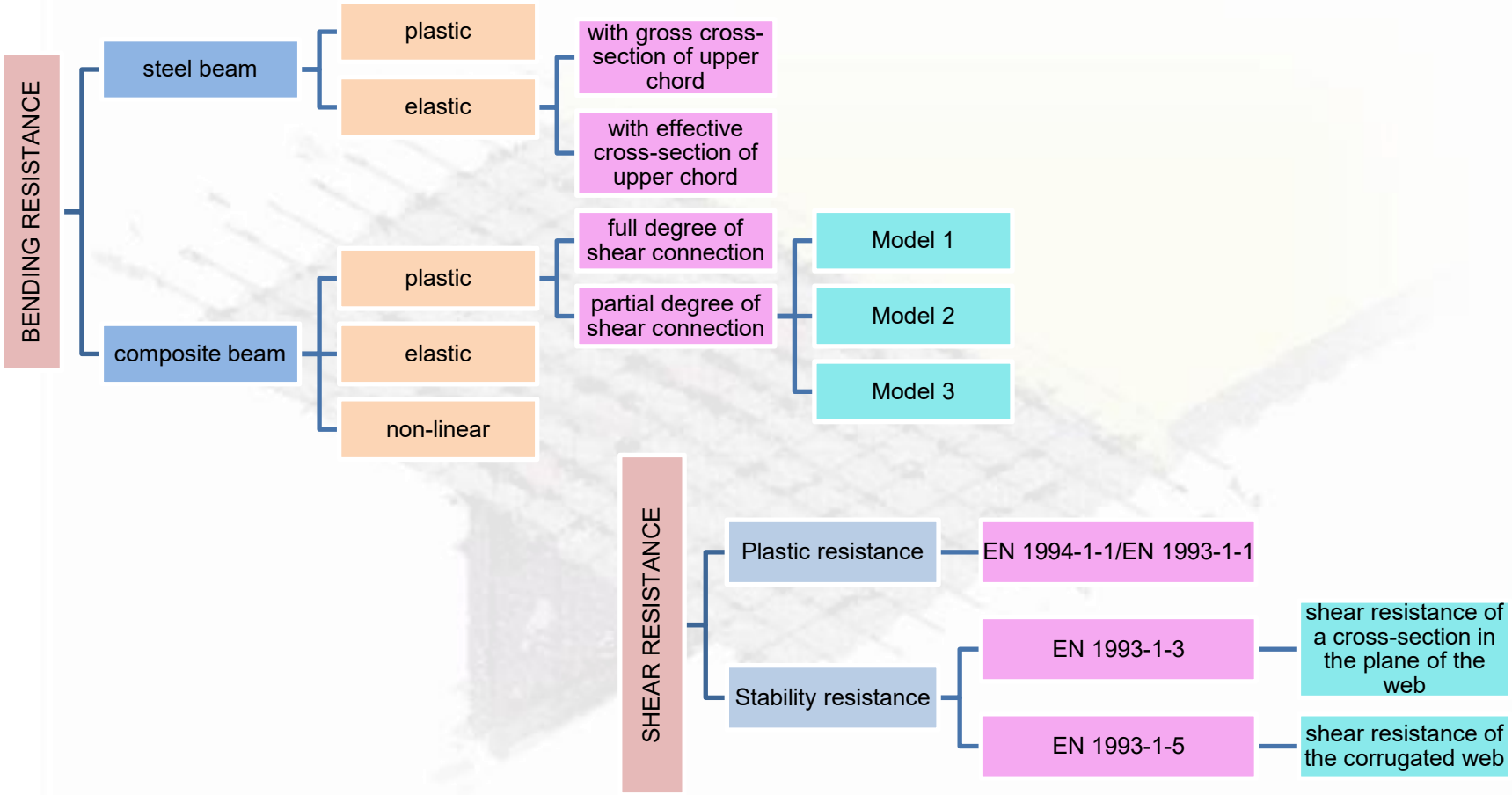

# Analytical proposals

## Bending resistance

### Bending resistance of steel beam – Plastic resistance EN 1993-1-1

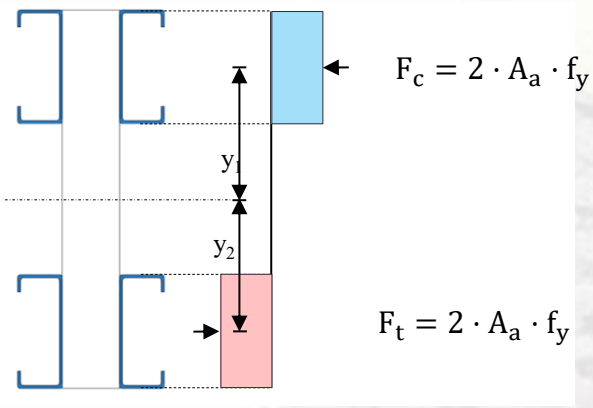


$$F_c = 2 \cdot A_a \cdot f_y$$

$$F_t = 2 \cdot A_a \cdot f_y$$

$$F_c = F_T$$

$$f_y \cdot 2 \cdot A_a = f_y \cdot 2 \cdot A_a$$

$$M_{pl,a} = f_y \cdot 2 \cdot A_a \cdot y_1 + f_y \cdot 2 \cdot A_a \cdot y_2$$

$$M_{pl,a} = f_y \cdot 2 \cdot A_a \cdot (y_1 + y_2)$$

| | Experiment - $M_{exp,a}$ [kNm] | Analytical – $M_{pl,a}$ [kNm] | $M_{pl,a}/M_{exp,a}$ |
|---|---|---|---|
| SB1 | 90.85 | 121.03 | 133% |
| SB2 | 79.12 | 117.6 | 149% |
| SB3 | 87.86 | 140.34 | 160% |

# Analytical proposals

## Bending resistance

### Bending resistance of steel beam – Elastic resistance EN 1993-1-1 / EN 1993-1-3

#### gross sectional properties

$$M_{el,a,red} = \frac{W_{eff,y} \cdot f_y}{\gamma_{M0}} \qquad W_{eff,y} = \frac{I_{y,eff,beam}}{h_{steelbeam}/2}$$

$$I_{y,beam} = 2 \cdot \left( 2 \cdot I_{y,a} + 2 \cdot A_a \cdot \left( \frac{h_{steelbeam}}{2} - \frac{h_a}{2} \right)^2 \right)$$

#### effective cross-section

$$M_{el,a,red} = \frac{W_{eff,y} \cdot f_y}{\gamma_{M0}} \qquad W_{eff,y} = \frac{I_{y,eff,beam}}{h_{steelbeam}/2}$$

$$I_{y,eff,beam} = 2 \cdot I_{y,eff,a} + 2 \cdot A_{a,eff} \cdot \left( \frac{h_{steelbeam}}{2} - \frac{h_a}{2} \right)^2 + 2 \cdot I_{y,a} + 2 \cdot A_a \cdot \left( \frac{h_{steelbeam}}{2} - \frac{h_a}{2} \right)^2$$

| | Experiment, $M_{exp,a}$ [kNm] | Analytical – $M_{el,a}$ [kNm] | $M_{el,a}/M_{exp,a}$ | Analytical – $M_{el,a,red}$ [kNm] | $M_{el,a,red}/M_{exp,a}$ |
|---|---|---|---|---|---|
| SB1 | 90.85 | 97.83 | 108% | 87.57 | 96% |
| SB2 | 79.12 | 91.74 | 116% | 87.36 | 110% |
| SB3 | 87.86 | 109.35 | 124% | 106.16 | 121% |

# Analytical proposals

## Bending resistance

### Bending resistance of a composite beam – Plastic resistance

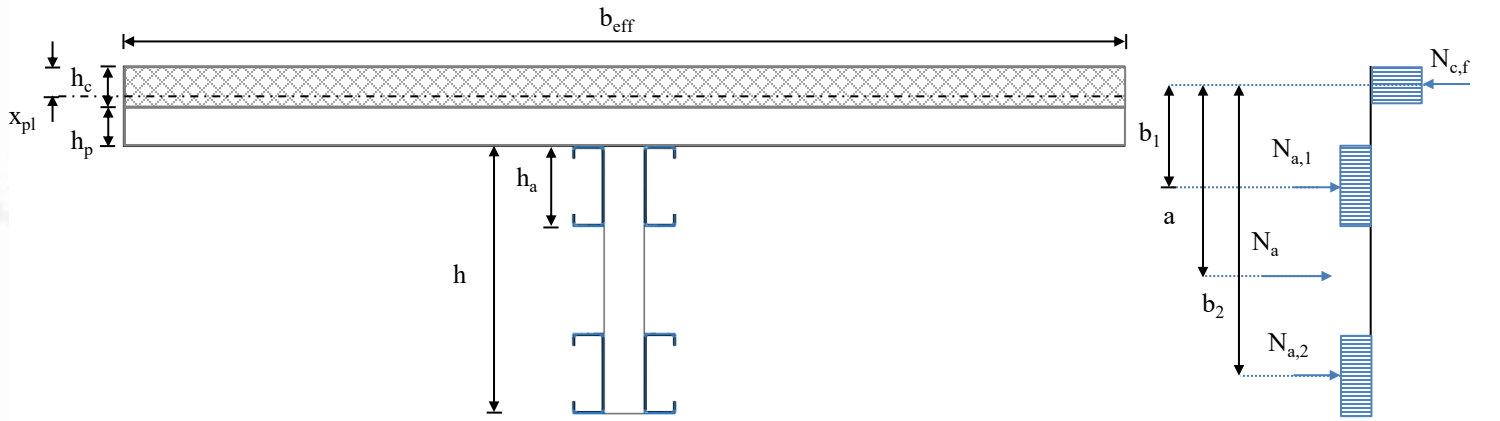


- full degree of shear connection
- the neutral axis positioned in the concrete slab

$$x_{pl} = \frac{4 \cdot A_a \cdot f_y}{b_{eff} \cdot 0.85 \cdot f_c}$$

$$M_{pl,full} = N_{c,f} \cdot a$$

$$M_{pl,full} = b_{eff} \cdot x_{pl} \cdot 0.85 \cdot f_c \cdot \left(\frac{h}{2} + h_c - \frac{x_{pl}}{2}\right)$$

$$M_{pl,full} = 2 \cdot A_a \cdot f_y \cdot b_1 + 2 \cdot A_a \cdot f_y \cdot b_2$$

$$M_{pl,full} = 2 \cdot A_a \cdot f_y \cdot \left(\frac{h_a}{2} + h_c + h_p - \frac{x_{pl}}{2}\right) + 2 \cdot A_a \cdot f_y \cdot \left(h - \frac{h_a}{2} + h_c + h_p - \frac{x_{pl}}{2}\right)$$

| | $A_a$ [mm2] | $h_a$ [mm] | h [mm] | $x_{pl}$ [mm] | $M_{pl,full}$ [kNm] |
|---|---|---|---|---|---|
| CB1 | 600 | 120 | 400 | 43.9 | 234.88 |
| CB2 | 455 | 120 | 500 | 33.3 | 211.28 |
| CB3 | 716 | 120 | 400 | 52.4 | 277.56 |

# Analytical proposals

## Bending resistance

### Bending resistance of a composite beam – Plastic resistance - Model 1 – Steel part resistance calculated by plastic model

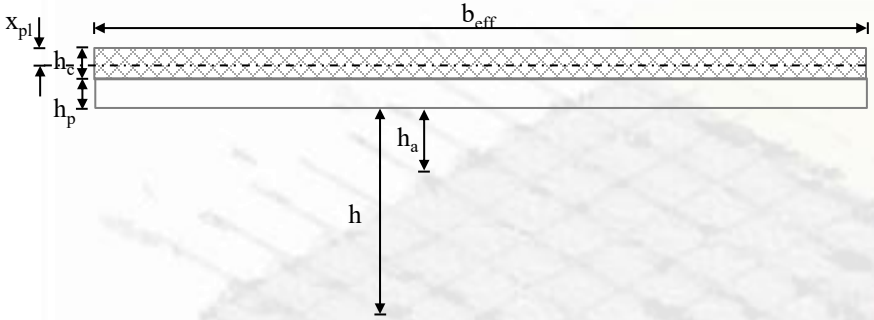


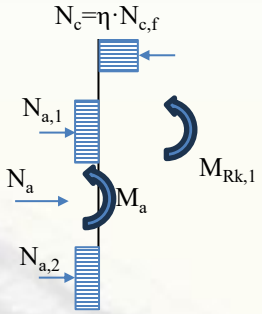


$$M_{Rk,1} = M_{pl,a} + (M_{pl,full} - M_{pl,a}) \cdot \eta$$

$$\alpha_b = 0.6 \cdot \left(\frac{34}{d}\right)^{0.23}$$

$$\alpha_c = \frac{22.5}{d+3} \leq 1.0$$

$$P_{c,Rk} = \frac{55 \cdot \alpha_c \cdot d^{1.9} \cdot \left(f_{ck} \cdot \frac{h_{sc}}{d}\right)^{0.4} + 22000}{\gamma_v}$$

### Bending resistance of a composite beam – Plastic resistance - Model 2 - steel part model calculated by the elastic model with gross cross-section of the upper chord

$$M_{Rk,2} = M_{el,a} + (M_{pl,full} - M_{el,a}) \cdot \eta$$

-neutral axis lies in the concrete slab or at the interface of the concrete slab and steel section, but the steel section is considered to have elastic behaviour

### Bending resistance of a composite beam – Plastic resistance - Model 3 - steel part model calculated by an elastic model with effective cross-section of upper chord

$$M_{Rk,3} = M_{el,a,red} + (M_{pl,full} - M_{el,a,red}) \cdot \eta$$

-neutral axis lies in the steel part of the cross-section between the upper and bottom channel profiles
-the effective cross-section of upper chord because of the compression in the upper channel profiles, bottom channel profiles are considered to have gross values of geometrical properties

# Analytical proposals

## Bending resistance

### Bending resistance of a composite beam – Elastic resistance

$$EI_L = E_a \cdot I_{i,L}$$

$$\sigma_a = E_a \cdot \frac{M_{Ek,a}}{EI_L} \cdot z_a$$

$$\sigma_c = E_c \cdot \frac{M_{Ek,c}}{EI_L} \cdot z_c$$

$$N_{c,el} = k \cdot \frac{M_{el,Rk}}{I_{i,L}} \cdot (A_{c,L} \cdot z_{ic,L})$$

$$z_{ic,L} = \frac{A_a \cdot a_a}{A_{i,L}}$$

$$\sigma_{a,II} = E_a \cdot \frac{M_{Ek,II,a}}{EI_L} \cdot z_a$$

$$\sigma_c = E_c \cdot \frac{M_{Ek,II,c}}{EI_L} \cdot z_c$$

$$M_{el} = M_a + k_{el} \cdot M_i$$

$$M_{el} = M_{Ek,I} + k \cdot M_{Ek,II}$$

### Bending resistance of a composite beam – Non-linear resistance

$$N_c \le N_{c,el} \rightarrow M_{non-linear} = M_a + (M_{el} - M_a) \cdot \frac{N_c}{N_{c,el}}$$

$$N_{c,el} \le N_c \le N_{c,f} \rightarrow M_{non-linear} = M_{el} + (M_{pl} - M_{el}) \cdot \frac{N_c - N_{c,el}}{N_{c,f} - N_{c,el}}$$

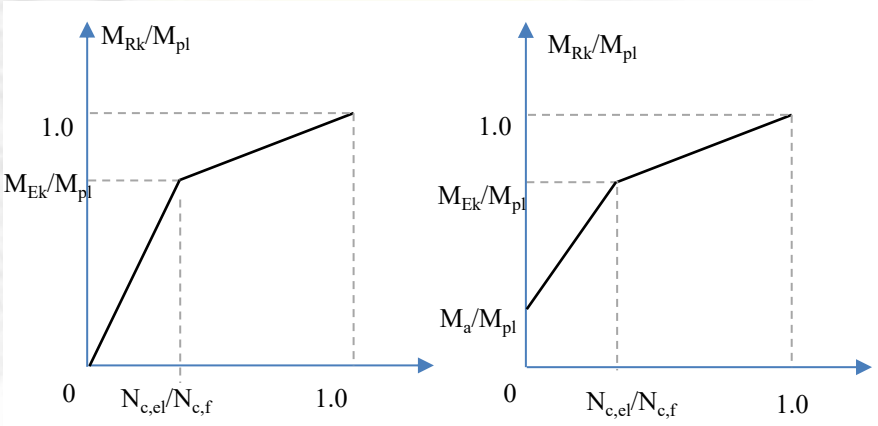

# Analytical proposals

## Bending resistance

Bending resistance of a composite beam – Comparison of experimental results with results of different analytical methods

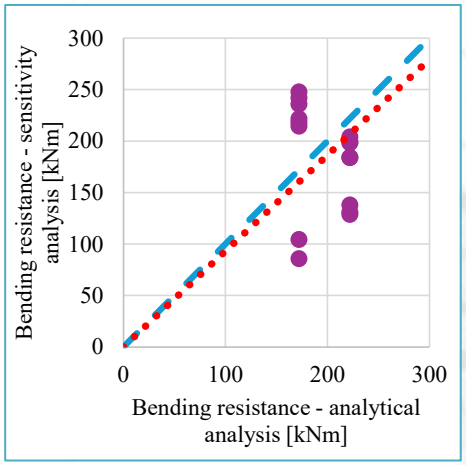


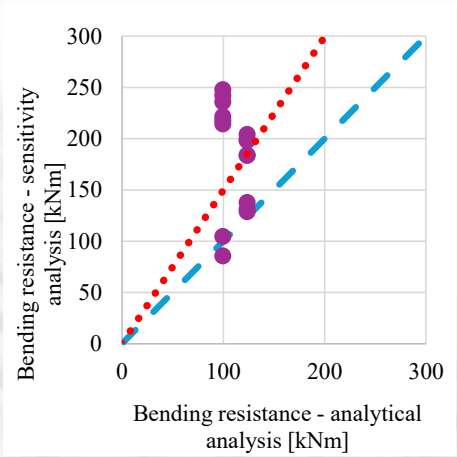


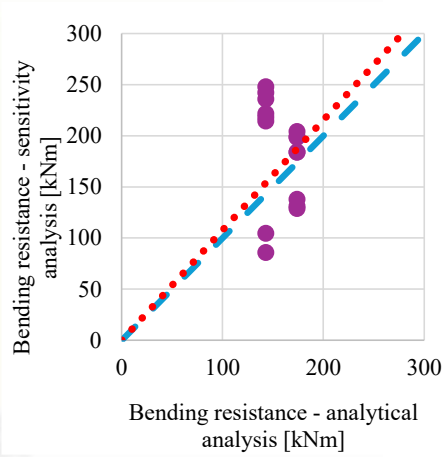


plastic model – Model 3

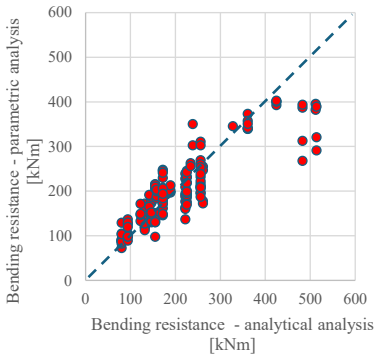


elastic method

$$M_{Rk} = 0.96 \cdot \left(M_{el,a,red} + \left(M_{pl,full} - M_{el,a,red}\right) \cdot \eta\right)$$

$$M_{Rk} = M_{el,a,red} + 0.90 \cdot \left(M_{pl,full} - M_{el,a,red}\right) \cdot \eta$$

non-linear model

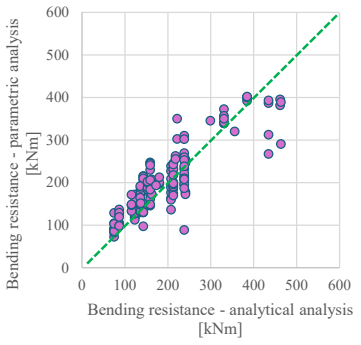

# Analytical proposals

## Bending resistance

Bending resistance of a composite beam – Comparison of experimental results with results of different analytical methods

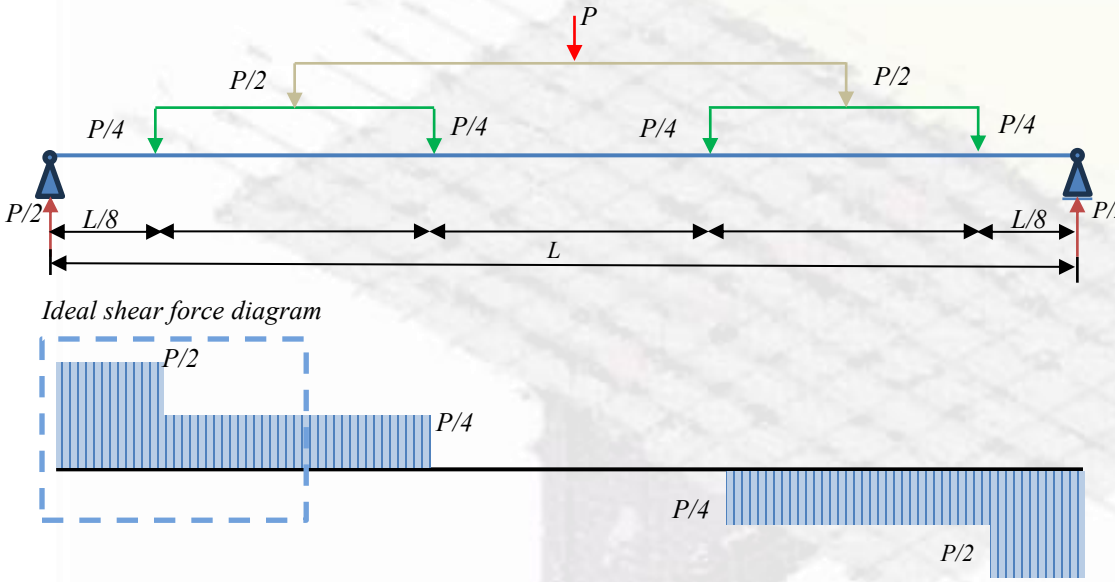


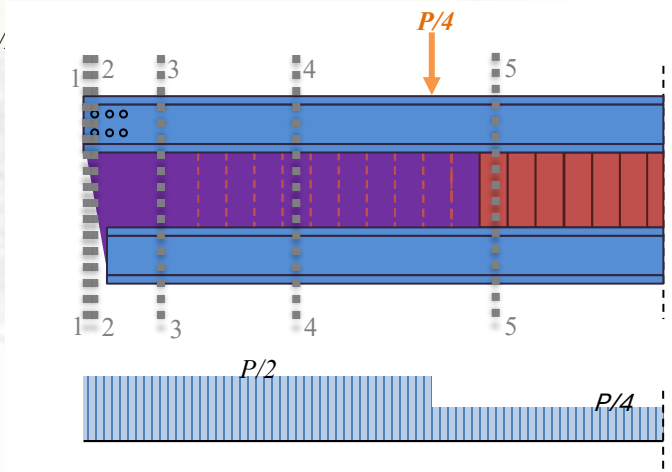


Internal forces along the beam and the arrangement of the considered cross-sections along the beam

# Analytical proposals

## Shear resistance

### Cross-sections for the shear resistance analysis of the LWT-FLOOR system

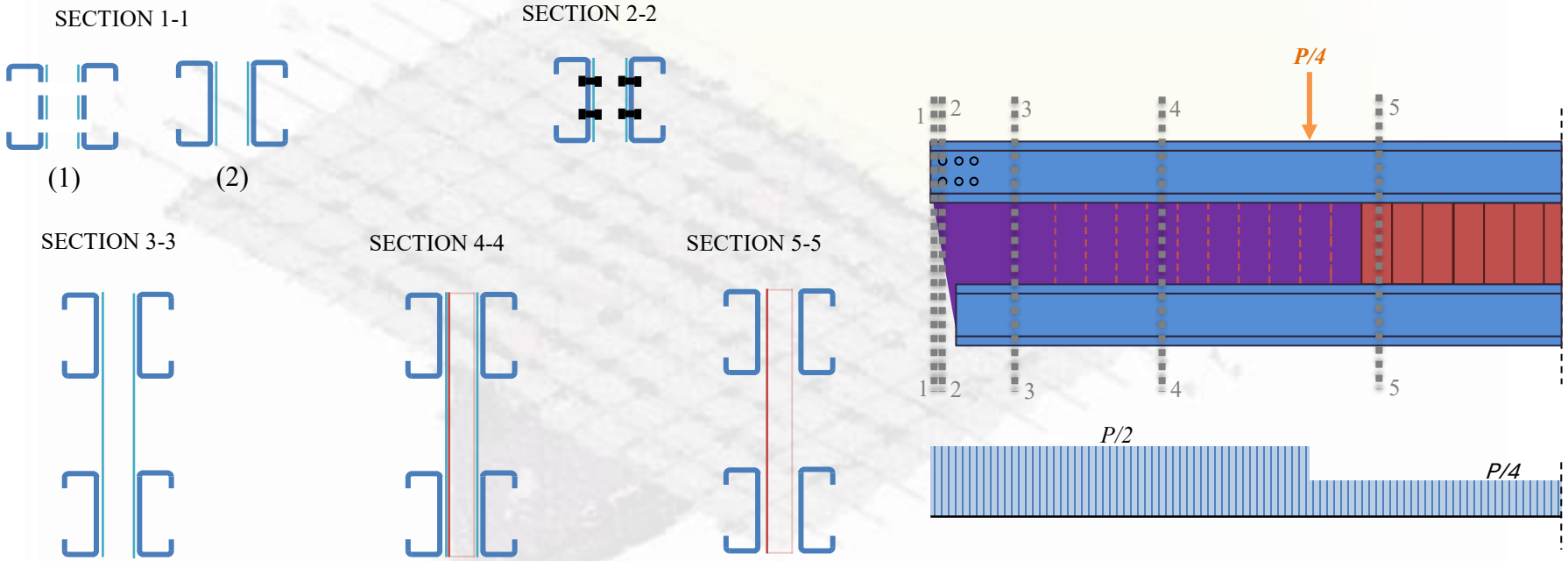

# Analytical proposals

## Shear resistance

### Verification of bearing shear resistance in cold-formed steel section for Section 2-2

$$F_{b,Rk} = \min\left(2.5 \cdot \alpha_b \cdot k_{tI} \cdot d \cdot t_I \cdot f_{u,I};\ 2.5 \cdot \alpha_b \cdot k_{tII} \cdot d \cdot t_{II} \cdot f_{u,II}\right)$$

$k_{tI} = (0.8 \cdot t_I + 1.5)/2.5$ for $0.75\ \text{mm} \leq t_I \leq 1.25\ \text{mm}$

$k_{tI} = 1.0$ for $t_I > 1.25\ \text{mm}$

$k_{tII} = (0.8 \cdot t_{II} + 1.5)/2.5$ for $0.75\ \text{mm} \leq t_{II} \leq 1.25\ \text{mm}$

$k_{tII} = 1.0$ for $t_{II} > 1.25\ \text{mm}$

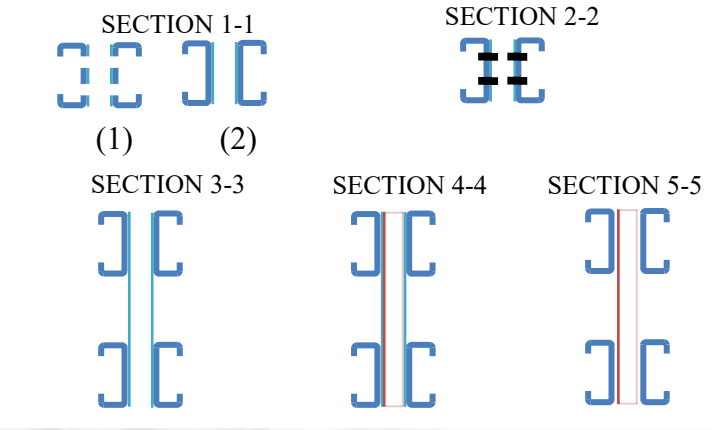


### Restrictions for the calculation

- not valid for beams that failed due to brittle failure of spot welds (interfacial fracture of the spot weld)
- essential to consider the number of welds connecting the steel sheets

# Analytical proposals

## Verification procedure

1. calculating the bending resistance of the system - determining the maximum force that occurs at the end of the composite beam
2. assumed number of welds

2.A the number of transverse welds is adjusted — either increased or decreased

2.B all welds should be positioned within the section of the C-profile located between lips, allowing welding device electrodes sufficient access to the weld area

3. models that failed in unfavourable way were identified and must therefore be excluded from further analysis

3.A sheet separation due to brittle failure because of thinner spot-welded sheets

3.B thicker sheets, where spot weld failure has also taken place; however, due to their greater thickness, the separated elements attempt to retain their original shape until they come into contact with the concrete slab, which then crushes them

models with corrugated web and shear plate thicknesses of 1.0 mm and 0.8 mm

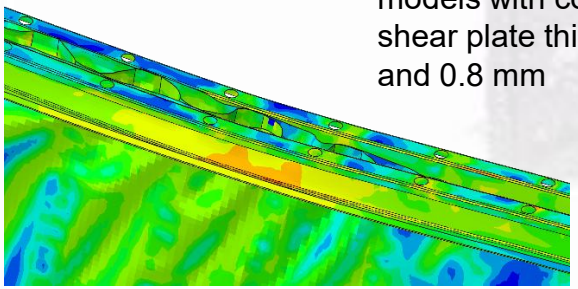

models with corrugated web and shear plate thicknesses of 1.0 mm and 1.5 mm, as well as their combinations

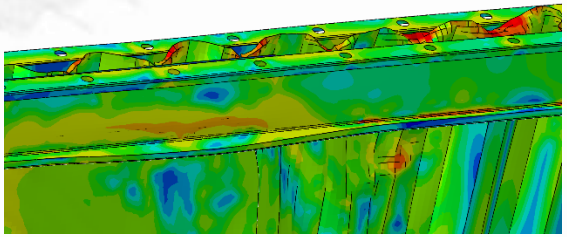

# Probabilistic analysis

## Calculation of the partial factor method based on design values - Partial factor of spot welds

| NAME | 1st group | 2nd group | 3rd group |
|---|---|---|---|
| SW 0.8-0.8 | 1.572 | 1.073 | 1.140 |
| SW 0.8-1.0 | | | 1.087 |
| SW 0.8-1.25 | | | 1.070 |
| SW 0.8-1.5 | | | 1.048 |
| SW 0.8-2.0 | | | 1.047 |
| SW 0.8-2.5 | | | 1.148 |
| SW 0.8-3.0 | | | 1.089 |
| SW 1.0-1.0 | | 1.094 | 1.060 |
| SW 1.0-1.25 | | | 1.043 |
| SW 1.0-1.5 | | | 1.063 |
| SW 1.0-2.0 | | | 1.036 |
| SW 1.0-2.5 | | | 1.027 |
| SW 1.0-3.0 | | | 1.047 |
| SW 1.25-1.25 | | 1.064 | 1.053 |
| SW 1.25-1.5 | | | 1.102 |
| SW 1.25-2.0 | | | 1.078 |
| SW 1.25-2.5 | | | 1.055 |
| SW 1.25-3.0 | | | 1.065 |
| SW 1.5-1.5 | | 1.067 | 1.022 |
| SW 1.5-2.0 | | | 1.234 |
| SW 1.5-2.5 | | | 1.049 |
| SW 1.5-3.0 | | | 1.136 |
| SW 2.0-2.0 | | 1.052 | 1.046 |
| SW 2.0-2.5 | | | 1.051 |
| SW 2.0-3.0 | | | 1.114 |
| SW 2.5-2.5 | | 1.047 | 1.051 |
| SW 2.5-3.0 | | | 1.074 |
| SW 3.0-3.0 | | 1.141 | 1.141 |

# Probabilistic analysis

## Partial factor of the analytical resistance model for bending of the analysed system

$$b\delta_i = \frac{r_{e,i}}{r_{t,i}}$$

$$r_m = b \cdot r_t(X_m) \cdot \delta = b \cdot g_{rt}(X_m) \cdot \delta$$

$$\Delta_i = \ln(b\delta_i) = \ln(r_{ei}) - \ln(r_{ti})$$

$$\bar{\Delta} = \frac{1}{n}\sum_{i=1}^{n} \Delta_i$$

$$s_\Delta^2 = \frac{1}{n-1}\sum_{i=1}^{n} (\Delta_i - \bar{\Delta})^2$$

$$b = \exp\left(\bar{\Delta} + \frac{1}{2}s_\Delta^2\right)$$

$$V_\delta = \sqrt{\exp(s_\Delta^2) - 1}$$

$$V_r^2 = (V_\delta^2 + 1)\left[\prod_{i=1}^{j}(V_{Xi}^2 + 1)\right] - 1$$

$$V_{rt} = \sqrt{\sum_{i=1}^{J} V_{xi}^2}$$

$$Q_{rt} = \sigma_{\ln(r_t)} = \sqrt{\ln(V_{rt}^2 + 1)}$$

$$Q_\delta = \sigma_{\ln(\delta)} = \sqrt{\ln(V_\delta^2 + 1)}$$

$$Q = \sigma_{\ln(r)} = \sqrt{\ln(V_r^2 + 1)}$$

$$\alpha_{rt} = \frac{Q_{rt}}{Q}$$

$$\alpha_\delta = \frac{Q_\delta}{Q}$$

The design value, $r_d$, equals 125.29 kNm while the characteristic value is 154.85 kNm. This leads to a partial factor of 1.236.

$$r_d = b \cdot g_{rt}(X_m) \cdot \exp(-k_{d,\infty} \cdot \alpha_{rt} \cdot Q_{rt} - k_{d,n} \cdot \alpha_\delta \cdot Q_\delta - 0.5 \cdot Q^2)$$

$$r_k = b \cdot g_{rt}(X_m) \cdot \exp(-k_\infty \cdot \alpha_{rt} \cdot Q_{rt} - k_n \cdot \alpha_\delta \cdot Q_\delta - 0.5 \cdot Q^2)$$

# Probabilistic analysis

## Calculation of the partial factor method based on design values – Model uncertainty factor

| PA1 | PA2 | PA3 |
|---|---|---|
| -Eurocode equation<br>- assuming a plastic stress distribution for partial shear connection and using partial factors provided in the standard | - newly proposed equation<br>- partial factors from the standard | - newly proposed equation<br>- calculated partial factor for the resistance |
| uncertainty of calculation resistance model, $\Theta_R$ | | |
| 1.06 | 1.10 | 1.10 |
| standard deviation | | |
| 0.22 | 0.23 | 0.23 |

# Probabilistic analysis

| Basic variable | Distribution | Mean value (mean) | standard deviation (σ) according to the literature | Considered mean value | Considered standard deviation (σ) |
|---|---|---|---|---|---|
| $W_y/W_{y,eff}$ | normal | $0.99 \cdot X_{nom}$ | 0.01 mean-0.04 mean | $0.99 \cdot X_{nom}$ | 0.025·mean |
| $f_y$ | lognormal | $f_{yk}+2 \cdot \sigma$ | 0.05 mean-0.08 mean | $f_{yk}+2 \cdot \sigma$ | 0.065·mean |
| $A_a/ A_{a,eff}$ | normal | $0.99 \cdot X_{nom}$ | 0.01 mean-0.04 mean | $0.99 \cdot X_{nom}$ | 0.025·mean |
| $h_a$ | normal | $h_{a,k}$ | 0.005-0.01 | $h_{a,k}$ | 0.0075 |
| $h_c$ | normal | $h_{c,k}$ | 0.005-0.01 | $h_{c,k}$ | 0.0075 |
| $h_p$ | normal | $h_{p,k}$ | 0.005-0.01 | $h_{p,k}$ | 0.0075 |
| $b_{eff}$ | normal | $b_{eff,k}$ | 0.005-0.01 | $b_{eff,k}$ | 0.0075 |
| $f_c$ | lognormal | $f_{ck}+2 \cdot \sigma$ | 0.05 mean-0.15 mean | $f_{ck}+2 \cdot \sigma$ | 0.1·mean |
| h | normal | $h_k$ | 0.005-0.01 | $h_k$ | 0.0075 |
| L | normal | L | 0.01 L | L | 0.01 L |
| $\Theta_E$ | normal | 1 | 0.05-0.1 | 1 | 0.075 |
| $\Theta_R$ | normal | 1.0-1.25 | 0.05-0.2 | 1.125 | 0.125 |
| G | normal | $G_k$ | 0.1 mean | Gk | 0.1 mean |
| Q | Gumbel | 0.6 $Q_k$ | 0.35 mean | 0.6 Qk | 0.35 mean |

# Probabilistic analysis

The calculation of factor Z for PA1 from the equation R-Z·E=0 is shown:

$$Z=\frac{\left(W_y\cdot\frac{f_y}{\gamma_{steel}}+0.7\cdot\left(\left(2\cdot A_a\cdot\frac{f_y}{\gamma_{steel}}\cdot\left(\frac{h_a}{2}+h_c+h_p-\frac{4\cdot A_a\cdot\frac{f_y}{\gamma_{steel}}}{2\cdot b_{eff}\cdot 0.85\cdot f_{ck}}\right)+2\cdot A_a\cdot\frac{f_y}{\gamma_{steel}}\cdot\left(h-\frac{h_a}{2}+h_c+h_p-\frac{4\cdot A_a\cdot\frac{f_y}{\gamma_{steel}}}{2\cdot b_{eff}\cdot 0.85\cdot f_{ck}}\right)-W_y\cdot\frac{f_y}{\gamma_{steel}}\right)\cdot\eta\right)\right)}{1.35\cdot\frac{L^2}{8}\cdot 1+1.5\cdot 2\cdot Q[\%]\cdot\frac{L^2}{8}}$$

Factor Z used for PA2 is shown by equation

$$Z=\frac{\left(W_{y,eff}\cdot\frac{f_y}{\gamma_{steel}}+0.7\cdot\left(\left(2\cdot A_{a,eff}\cdot\frac{f_y}{\gamma_{steel}}\cdot\left(\frac{h_a}{2}+h_c+h_p-\frac{\left(2\cdot A_{a,eff}\cdot\frac{f_y}{\gamma_{steel}}\right)+\left(2\cdot A_a\cdot\frac{f_y}{\gamma_{steel}}\right)}{2\cdot b_{eff}\cdot 0.85\cdot f_{ck}}\right)+2\cdot A_{a,eff}\cdot\frac{f_y}{\gamma_{steel}}\cdot\left(h-\frac{h_a}{2}+h_c+h_p-\frac{\left(2\cdot A_{a,eff}\cdot\frac{f_y}{\gamma_{steel}}\right)+\left(2\cdot A_a\cdot\frac{f_y}{\gamma_{steel}}\right)}{2\cdot b_{eff}\cdot 0.85\cdot f_{ck}}\right)-W_{y,eff}\cdot\frac{f_y}{\gamma_{steel}}\right)\cdot\eta\right)\right)}{1.35\cdot\frac{L^2}{8}\cdot 1+1.5\cdot 2\cdot Q[\%]\cdot\frac{L^2}{8}}$$

For PA3, which uses global partial factor, design factors Z are calculated by:

$$Z_3=\frac{\left(W_{y,eff}\cdot f_y+0.9\cdot\left(\left(\begin{array}{l}2\cdot A_a\cdot f_y\cdot\left(\frac{h_a}{2}+h_c+h_p-\frac{4\cdot A_a\cdot f_y}{2\cdot b_{eff}\cdot 0.85\cdot f_c}\right)+\\+2\cdot A_a\cdot f_y\cdot\left(h-\frac{h_a}{2}+h_c+h_p-\frac{4\cdot A_a\cdot f_y}{2\cdot b_{eff}\cdot 0.85\cdot f_c}\right)-\\-W_{y,eff}\cdot f_y\end{array}\right)\cdot\eta\right)\right)/\gamma_{global}}{1.35\cdot\frac{L^2}{8}\cdot 1+1.5\cdot 2\cdot Q[\%]\cdot\frac{L^2}{8}}$$

# Probabilistic analysis

Several cases were analysed to account for the uncertainty and different ratios regarding the live load, Q, and the permanent load, G. In each case, the permanent load was taken as 100%. The equation used to define the ratio of the live load to permanent load is

$$r = \frac{Q}{G+Q}$$

Considered values of permanent and variable load

| r | 0.3 | 0.4 | 0.5 | 0.6 | 0.66 | 0.7 | 0.75 | 0.8 |
|---|---|---|---|---|---|---|---|---|
| G [%] | 100 | 100 | 100 | 100 | 100 | 100 | 100 | 100 |
| Q [%] | 21 | 33 | 50 | 75 | 100 | 117 | 150 | 200 |

# Probabilistic analysis

PA1

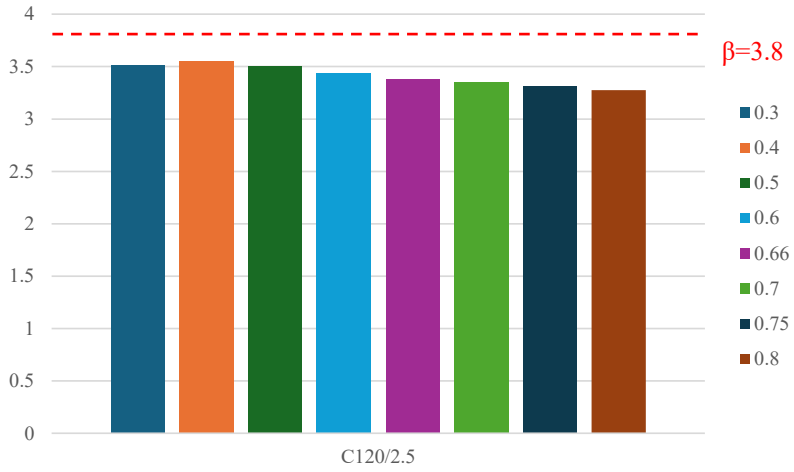


PA2

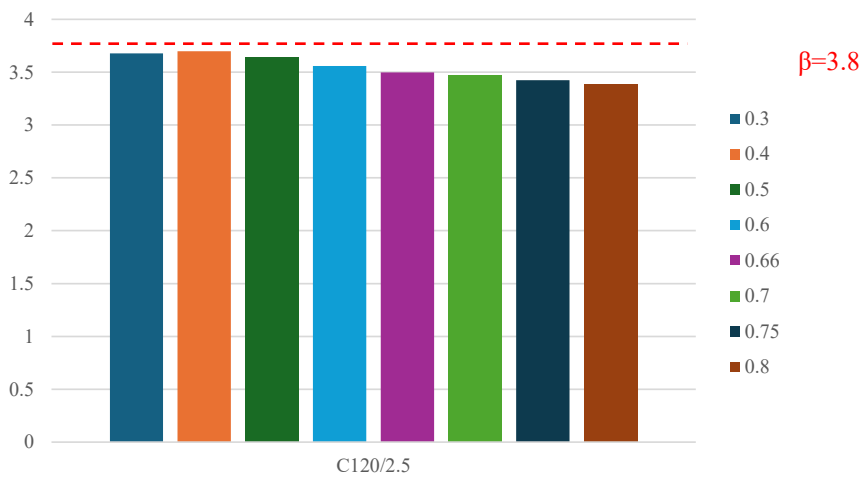


Reliability indices for approaches PA1, PA2 and PA3 – C120/2.5 – 6m

PA3

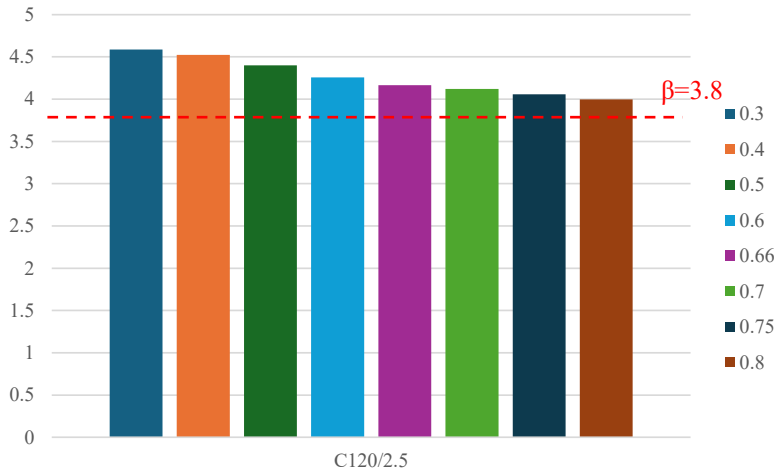

# Probabilistic analysis

PA1

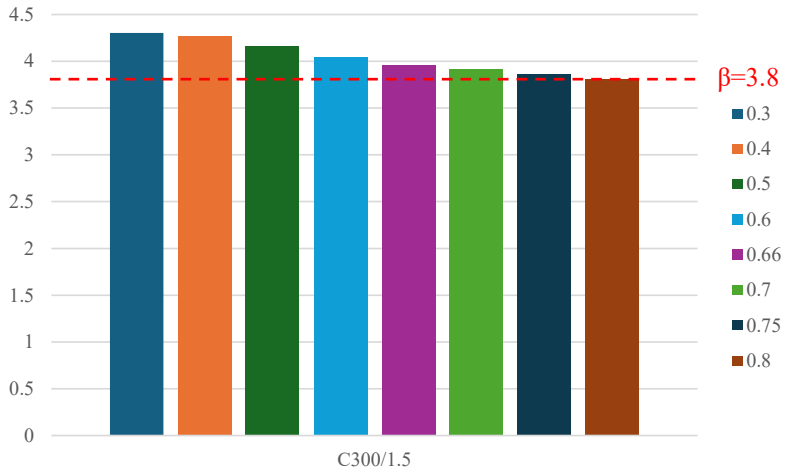


PA2

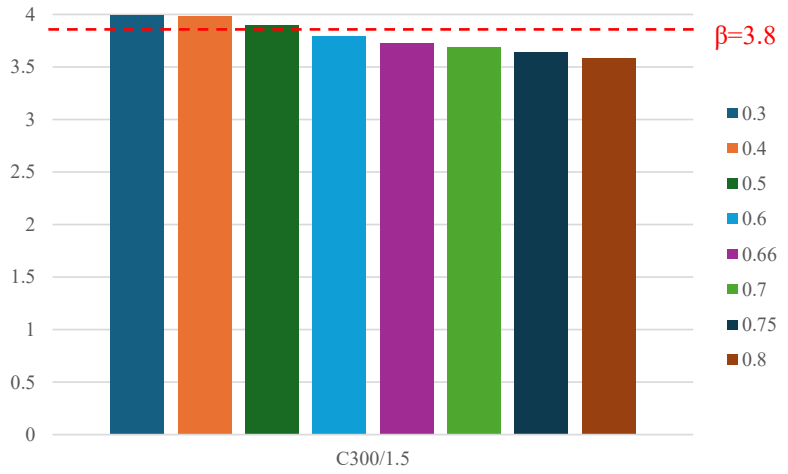


Reliability indices for approaches PA1, PA2 and PA3 –C300/1.5 – 15 m

PA3

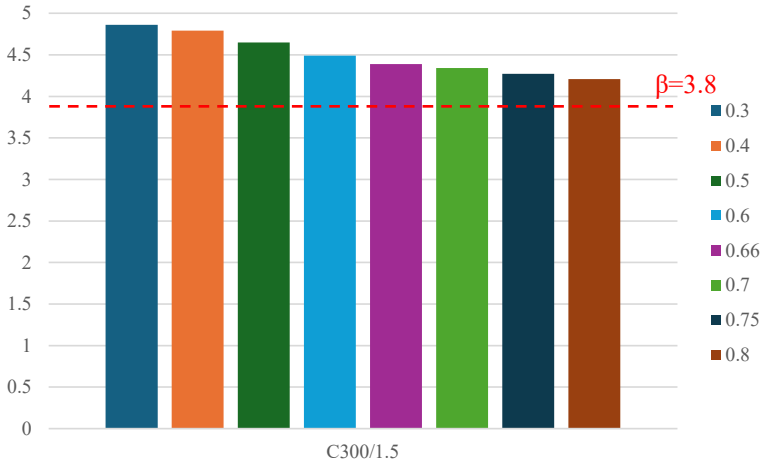

# Conclusions

## Scientific contribution of research

- nonlinear numerical models of composite floor system that were developed using the finite element method and evaluated based on the results of laboratory tests,
- identification and characterisation of local and global failure mechanisms of the composite floor system,
- developed analytical design procedures for the composite floor system subjected to bending moment and shear force,
- determination of statistical parameters of basic variables on the resistance side of the composite floor system,

evaluation of analytical design procedures using probabilistic methods

## Objectives

- ✓ to collect and analyse existing reliability verification procedures for composite beams
- ✓ to analyse laboratory test results with the identification of failure modes
- ✓ to develop and calibrate numerical models based on test results
- ✓ to validate deterministically and probabilistically analytical models
- ✓ to develop a reliable design procedure for the analysed system

## Hypothesis

**H1:** The application of built-up cold-formed steel beams in a composite structure with reinforced concrete slab can replace hot-rolled steel beams with reduced steel consumption

**H2:** Spot welds and demountable shear connectors will provide a reliable connection between elements of the system.

# Conclusions

Experimental results highlighted the importance of the interaction between steel section geometry, material thickness, and weld detailing in determining the load-bearing capacity and failure modes of the system. Among the tested steel beams,

- SB1 demonstrated the highest capacity due to a **smart selection of section height and material thickness**
- SB2 failed from local buckling owing to its thinner components
- SB3, despite having the thickest elements, failed due to spot weld failure, emphasising the critical role of weld detailing in system performance.
- CB2 exhibited the highest load capacity, primarily due to its higher steel section,
- CB3 achieved the lowest capacity due to **spot weld failure**, again underscoring the importance of weld performance.
- Mid-span deflection, local buckling, and shear failure mechanisms were strongly influenced by variations in section height, thickness, and spot weld design.

# Conclusions

The thickness of the channel profile emerged as a dominant factor influencing flexural resistance.

Enhancements in the thickness of the corrugated web and shear plates also contributed to improved bending capacity, primarily due to increased stiffness and delay in local buckling.

The arrangement and quantity of shear connectors in the concrete slab had a significant effect on bending performance. An increased number of shear connectors resulted in greater composite action and overall capacity. A notable distinction was observed in the influence of shear connector diameter.

The role of spot weld configuration was found to be span-dependent.

Finally, the shape of web openings affected bending capacity only in models with corrugated web thicknesses of 1.5 mm or more. For thinner webs (0.8–1.0 mm), differences between circular and rectangular openings were negligible.

As the beam span increases, and assuming the use of thicknesses sufficient to prevent brittle failure of spot welds, the bending capacity of the composite beam correspondingly improves. However, it is crucial to avoid using thin elements, particularly in regions subjected to high shear forces, such as shear plates, as they may lead to excessive deformation and premature beam failure.

# Conclusions

## Recommendations for further research

-investigate in more detail the influence of sheet thickness on the load-bearing capacity of the composite system
↓
-sheet thicknesses affect the characteristics of spot welds' resistance, thereby expanding the knowledge of their behaviour as well

-to include other types of steel, including high-strength steels

-to consider other types of sheeting profiles as well

-influence of different rib arrangements in the corrugated web

-alternative methods of connecting steel sheets, such as MIG brazing or riveting

-testing beams with reinforcements around the web openings

Given that the shear connection plays a significant role in the resistance model, it is first necessary to investigate its influence in more detail, especially considering that the conducted studies employed expressions for the resistance of headed shear studs to reflect the actual behaviour of the demountable shear connection realised with bolts

# Reliability of composite steel - concrete floor system made of built-up cold-formed steel elements

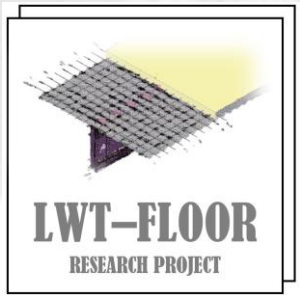



University of Zagreb/Faculty of Civil Engineering
http://www.grad.unizg.hr/lwtfloor